Aus der Poliklinik für Zahnärztliche Prothetik

der Ludwig-Maximilians-Universität München

3D-Druck des Hochleistungskunststoffes Polyetheretherketon (PEEK)

Dissertation

zum Erwerb des Doktorgrades der Zahnmedizin

an der Medizinischen Fakultät der

Ludwig-Maximilians-Universität zu München

vorgelegt von

Alexander Prechtel

aus

München

2020

Mit Genehmigung der Medizinischen Fakultät der Universität München

Erster Gutachter:	Prof. Dr. Dipl.-Ing. (FH) Bogna Stawarczyk, M.Sc.
Zweiter Gutachter:	Prof. Dr. med. dent. Daniel Edelhoff
Dritter Gutachter:	Prof. Dr. med. dent. Andrea Wichelhaus
Mitbetreuung durch den promovierten Mitarbeiter:	Dr. med. dent. Marcel Reymus
Dekan:	Prof. Dr. med. dent. Reinhard Hickel
Tag der mündlichen Prüfung:	04.06.2020

LMU LUDWIG-MAXIMILIANS-UNIVERSITÄT MÜNCHEN

Promotionsbüro
Medizinische Fakultät

MMRS

Eidesstattliche Versicherung

Prechtel, Alexander

Name, Vorname

Ich erkläre hiermit an Eides statt,

dass ich die vorliegende Dissertation mit dem Titel

3D-Druck des Hochleistungskunststoffes Polyetheretherketon (PEEK)

selbständig verfasst, mich außer der angegebenen keiner weiteren Hilfsmittel bedient und alle Erkenntnisse, die aus dem Schrifttum ganz oder annähernd übernommen sind, als solche kenntlich gemacht und nach ihrer Herkunft unter Bezeichnung der Fundstelle einzeln nachgewiesen habe.

Ich erkläre des Weiteren, dass die hier vorgelegte Dissertation nicht in gleicher oder in ähnlicher Form bei einer anderen Stelle zur Erlangung eines akademischen Grades eingereicht wurde.

München, den 14.01.2020	Alexander Prechtel
Ort, Datum	Unterschrift Doktorandin bzw. Doktorand

Meinen liebevollen Eltern & Schwester

Inhaltsverzeichnis

1. Einleitung und Zielsetzung..... 1

2. Publikationsliste..... 4

3. Eigene Arbeiten..... 5

3.1 Originalarbeit: Prechtel A, Reymus M, Edelhoff D, Hickel R, Stawarczyk B. Comparison of various 3D printed and milled PAEK materials: Effect of printing direction and artificial aging on Martens parameters. Dent Mater 2020;36:197-209 (https://doi.org/10.1016/j.dental.2019.11.017) IF 2018: 4.440..... 5

3.2 Originalarbeit: Prechtel A, Stawarczyk B, Hickel R, Edelhoff D, Reymus M. Fracture load of 3D printed PEEK inlays compared with milled ones, direct resin composite fillings, and sound teeth. Clin Oral Investig 2020; [epub 27.01.2020] (https://doi.org/10.1007/s00784-020-03216-5) IF 2018: 2.453..... 20

4. Diskussion..... 32

4.1 Vergleich der Martensparameter von 3D-gedruckten und gefrästen PAEK Materialien in Bezug auf Druckrichtung und künstlicher Alterung..... 32

4.2 Bruchlast von 3D-gedruckten PEEK Inlays im Vergleich zu gefrästen PEEK Inlays, direkten Komposit-Füllungen und nicht restaurierten Zähnen..... 38

5. Zusammenfassung und Ausblick..... 44

6. Englische Zusammenfassung..... 46

7. Literaturverzeichnis..... 48

8. Danksagung..... 55

1. Einleitung und Zielsetzung

Die Möglichkeit dreidimensional (3D) zu drucken und mit einer additiven Fertigungstechnologie (AM) Objekte schichtweise herzustellen, kann als Teil einer neuen industriellen Ära angesehen werden. AM hat das Potential traditionelle Entwicklungs- und Herstellungsprozesse dauerhaft zu verändern und in der modernen Industrie 4.0 zukünftig ein integraler Bestandteil zu werden. Die Anwendungsgebiete sind sehr vielfältig und es kommen durch die Entwicklung neuer Materialien, Technologien und auslaufender Patente fast täglich neue hinzu. In vielen Branchen wird der 3D-Druck bereits erfolgreich eingesetzt und ist nicht mehr wegzudenken, wie beispielsweise in der Automobilindustrie, in der Luft- und Raumfahrt, im Maschinen- und Modellbau sowie in medizinischen Bereichen [1]. Allerdings haben medizinische Anwendungen spezielle Anforderungen, wie eine hohe Komplexität, eine individuelle Anpassung an patientenspezifische Bedürfnisse, eine geringe Produktionsmenge, eine hohe Präzision sowie die Erfüllung der Richtlinien des Medizinproduktegesetzes.

Auch in der Zahnmedizin hat die additive Fertigung seit den 1980er Jahren Einzug gehalten und steht der bereits etablierten subtraktiven Technologie konkurrierend gegenüber [2]. Beide Verfahren sind ein Bestandteil der modernen Zahnheilkunde beziehungsweise Zahntechnik, bei denen ein digitaler Workflow mit Datenerhebung (beispielsweise durch eine intraorale Aufnahme mit einem 3D-Scanner), computerunterstützter Konstruktion (Computer-Aided-Design, CAD) und additiver respektive subtraktiver Fertigung (Computer-Aided-Manufacturing, CAM) vorzufinden sind.

Der 3D-Druck überzeugt mit zahlreichen Vorzügen, vor allem dadurch, dass Objekte mit komplexen individuellen Geometrien in einer kurzen Entwicklungs- und Produktionszeit kosteneffizient hergestellt werden können, da kein wesentlicher Materialverlust auftritt [3]. Nachteilig sind der umfangreiche Workflow mit einem technischen Verständnis, eine erforderliche Nachbearbeitung des gedruckten Bauteils (Postprocessing) sowie eine noch unzureichende klinische (Langzeit-) Erfahrung zu nennen.

Es werden inzwischen viele verschiedene Materialien für den 3D-Druck in der Zahnmedizin angeboten, wie zum Beispiel Wachse, Harze, Kunststoffe, Metalllegierungen und neuerdings Keramiken [4, 5].

Auch bei den in der Zahnheilkunde angewandten additiven Technologien gibt es eine große Auswahl an Möglichkeiten, wobei das Digital Light Processing (DLP), die Stereolithographie (SLA), das selektive Lasersintern (SLS), das Photopolymer Jetting (PJ) und das Fused Layer Manufacturing (FLM) hauptsächlich zur Anwendung kommen [6].

Letzteres ist seit 2013 dazu geeignet moderne Hochleistungskunststoffe aus der Gruppe der Polyaryletherketone (PAEK) additiv zu verarbeiten [7], wobei Polyetheretherketon (PEEK) als teilkristalliner thermoplastischer Kunststoff bisher in der Zahnmedizin am häufigsten als metall- und restmonomerfreie Alternative sowohl für festsitzenden als auch herausnehmbaren Zahnersatz, Implantat-Abutments und darüber hinaus bereits erfolgreich als eine Alternative zu den als „Goldstandard" titulierten Titanimplantaten verwendet wird [8]. Auch in anderen zahnmedizinischen Fachdisziplinen wie der Mund-, Kiefer- und Gesichtschirurgie sowie der Kieferorthopädie ist PAEK bereits erfolgreich im Einsatz [9].

Die hervorragende Biokompatibilität, das niedrige spezifische Gewicht, die Radiotransluzenz, ein knochenähnliches niedriges Elastizitätsmodul (E-Modul) von 4 GPa und optimale mechanische Eigenschaften sorgen für eine ausgesprochene hohe klinische Leistungsfähigkeit [10].

Um die Mechanik von dentalen Werkstoffen evaluieren zu können, stehen verschiedene Messmethoden zur Verfügung. So sind Härtemessungen maßgeblich dazu geeignet die Stabilität und Beständigkeit eines Werkstoffs zu ermitteln. Das Verfahren der Martenshärte (HM) Messung ist besonders für kunststoffbasierte Materialien prädestiniert, da diese Messmethodik Informationen über die plastische und elastische Verformung liefert [11].

Weibull Statistiken können in der dentalen Werkstoffkundeforschung zum Verständnis der strukturellen Zuverlässigkeit angewendet werden, wobei vor allem der Weibull-Modul ein Maß für die Streuung (Zuverlässigkeit) der mechanischen Festigkeit darstellt [12]. Zur Beurteilung der Struktur eines Werkstoffs dienen außerdem optische Untersuchungen, beispielsweise mittels Lichtmikroskopie.

Um die Langzeitbeständigkeit und das Verhalten von Werkstoffen nach Alterungsprozessen vorhersagen zu können, sind das Temperaturwechselbad, die Dampfsterilisation und die Kausimulation geeignete Methoden, um in vitro die klinische Situation adäquat nachzuahmen [13].

Allerdings ist die Datenlage über die mechanischen Eigenschaften und die Resistenz gegenüber mechanischen und thermischen Belastungen von in der FLM Technologie hergestellten PEEK Komponenten noch sehr rar, da bislang PEEK Werkstücke in der Zahnmedizin aus Granulat oder Pellets gepresst sowie CAD/CAM-basierend aus industriell vorgefertigten Ronden gefräst worden sind.

Aus diesem Grund setzt sich die vorliegende Arbeit mit dem 3D-Druck von PEEK in der FLM Technologie auseinander und untersucht zusammenfassend folgende Aspekte:

1. Vergleich der Martensparameter von 3D-gedruckten und gefrästen PAEK Materialien in Bezug auf Druckrichtung und künstlicher Alterung.

2. Bruchlast von 3D-gedruckten PEEK Inlays im Vergleich zu gefrästen PEEK Inlays, direkten Komposit-Füllungen und nicht restaurierten Zähnen.

2. Publikationsliste

Prechtel A, Reymus M, Edelhoff D, Hickel R, Stawarczyk B. Comparison of various 3D printed and milled PAEK materials: Effect of printing direction and artificial aging on Martens parameters. Dent Mater 2020;36:197-209 (https://doi.org/10.1016/j.dental.2019.11.017)

IF 2018: 4.440

Prechtel A, Stawarczyk B, Hickel R, Edelhoff D, Reymus M. Fracture load of 3D printed PEEK inlays compared with milled ones, direct resin composite fillings, and sound teeth. Clin Oral Investig 2020; [epub 27.01.2020] (https://doi.org/10.1007/s00784-020-03216-5)

IF 2018: 2.453

3. Eigene Arbeiten

Nachfolgend werden zwei Originalarbeiten in englischer Sprache vorgestellt und zusammengefasst.

3.1 Originalarbeit: Prechtel A, Reymus M, Edelhoff D, Hickel R, Stawarczyk B. Comparison of various 3D printed and milled PAEK materials: Effect of printing direction and artificial aging on Martens parameters. Dent Mater 2020;36:197-209 (https://doi.org/10.1016/j.dental.2019.11.017) IF 2018: 4.440´

Zusammenfassung

Ziel: Das Ziel dieser Untersuchung war es, den Einfluss einer künstlichen Alterung auf die Martensparameter von verschiedenen 3D-gedruckten und gefrästen PAEK Werkstoffen zu ermitteln.

Material und Methode: Es wurden insgesamt 120 Prüfkörper aus vier unterschiedlichen PEEK Materialien (Essentium PEEK (ESS), KetaSpire PEEK MS-NT1 (KET), VICTREX PEEK 450G (VIC) und VESTAKEEP i4G (VES)) mittels FLM Technologie additiv hergestellt. Dabei wurden je Material 15 Prüfkörper in horizontaler und vertikaler Druckrichtung gefertigt. Von den industriell fabrizierten PAEK Ronden (breCAM.BioHPP (BHD/ BHW), Dentokeep (DEN), JUVORA Dental Disc 2 (JUV) und Ultaire AKP (ULT)) wurden ebenfalls jeweils 15 Prüfkörper herausgefräst (n=75). Anschließend wurden die Martenshärte (HM), die Eindringhärte (H_{IT}) und der Eindringmodul (E_{IT}) vor und nach einer künstlichen Alterung durch ein Temperaturwechselbad (5-55 °C, 10.000 Thermozyklen) und einer Dampfsterilisation (134 °C, 2 bar) gemessen. Zusätzlich wurde jeweils die Oberflächenbeschaffenheit der Prüfkörper auf Veränderungen durch diese Alterung lichtmikroskopisch begutachtet.

Die ermittelten Daten wurden mittels Kolmogorov-Smirnov Test, einfaktorieller ANOVA mit anschließendem post-hoc Scheffé Test und partiellem Eta-Quadrat sowie mittels Kruskal-Wallis-, Mann-Whitney-U-, Friedmann- und Wilcoxon-Test ausgewertet. Dabei wurde jeweils ein Wert von $p<0,05$ als signifikant angesehen.

Ergebnisse: Im Allgemeinen zeigten die gefrästen Prüfkörper höhere Martensparameter als die gedruckten Prüfkörper ($p<0,001$). Die künstliche Alterung hatte auf die gemessenen Parameter einen negativen Einfluss ($p<0,001$). In horizontaler Richtung gedruckte Prüfkörper hatten unabhängig vom Material und dem Alterungsprozess höhere Martensparameter als die in vertikaler Richtung gedruckten Varianten ($p<0,001$). ESS und BHD lieferten von allen untersuchten PAEK Werkstoffen sowohl vor der Alterung als auch nach dem Temperaturwechselbad und der Dampfsterilisation die höchsten Werte, während bei VIC und ULT die Werte am geringsten waren ($p<0,001$).
Die lichtmikroskopischen Untersuchungen zeigten keine größeren Veränderungen der Materialien durch die künstliche Alterung.

Schlussfolgerung: 3D-gedruckte PEEK Materialien zeigten geringere Martensparameter als die gefrästen Werkstoffe, wobei die in horizontaler Richtung gedruckten Prüfkörper höhere Werte aufwiesen als die in vertikaler Richtung gedruckten Varianten. Die künstliche Alterung stellte zwar einen negativen Einflussfaktor auf die Martensparameter dar, hatte jedoch keinen wesentlichen Einfluss auf die Beschaffenheit der Prüfkörperoberfläche.

Klinische Relevanz: Bei der additiven Verarbeitung von PEEK Materialien mittels FLM Technologie haben Druckrichtung und Alterungsprozesse einen fundamentalen Einfluss auf die mechanischen Eigenschaften der gedruckten Bauteile.

DENTAL MATERIALS 36 (2020) 197–209

Available online at www.sciencedirect.com

ScienceDirect

journal homepage: www.intl.elsevierhealth.com/journals/dema

Comparison of various 3D printed and milled PAEK materials: Effect of printing direction and artificial aging on Martens parameters

Alexander Prechtel[a,*,1], *Marcel Reymus*[b,1], *Daniel Edelhoff*[a], *Reinhard Hickel*[b], *Bogna Stawarczyk*[a]

[a] *Department of Prosthetic Dentistry, LMU Munich, Goethestrasse 70, Munich, 80336, Germany*
[b] *Department of Conservative Dentistry and Periodontology, LMU Munich, Goethestrasse 70, Munich, 80336, Germany*

ARTICLE INFO

Article history:
Accepted 15 November 2019

Keywords:
PAEK
3D printing
Additive manufacturing
Fused layer manufacturing (FLM)
Martens parameters
Thermocycling/autoclaving

ABSTRACT

Objectives. The aim of this study was to investigate the effect of artificial aging on the Martens parameters of different 3D printed and milled polyaryletherketon (PAEK) materials.

Methods. In total 120 specimens of 4 different polyetheretherketon (PEEK) materials (Essentium PEEK, KetaSpire PEEK MS-NT1, VICTREX PEEK 450 G and VESTAKEEP i4 G) were additively manufactured via fused layer manufacturing (FLM) in either horizontal or vertical directions (n = 15 per group). 75 specimens were milled out of prefabricated PAEK blanks from the materials breCAM.BioHPP, Dentokeep, JUVORA Dental Disc 2 and Ultaire AKP (= 15 per group). Martens hardness (HM), indentation hardness (H_{IT}) and indentation modulus (E_{IT}) were determined initially and longitudinally after thermocycling (5–55 °C, 10,000x) and autoclaving (134 °C, 2 bar). In each case, the surface topography of the specimens was examined for modifications using a light microscope.

Data were analysed with Kolmogorov-Smirnov test, univariate ANOVA followed by post-hoc Scheffé test with partial eta squared (η_p^2), Kruskal–Wallis-, Mann–Whitney-U-, Friedman- and Wilcoxon-Test. A value of $p < 0.05$ was considered as significant.

Results. Milled specimens showed higher Martens parameters than printed ones ($p < 0.001$). Artificial aging had a negative effect on the measured parameters ($p < 0.001$). Horizontally printed specimens presented higher Martens parameters than vertically printed ones, regardless of material and aging process ($p < 0.001$). Essentium PEEK and breCAM.BioHPP showed the highest and VICTREX PEEK 450G as well as Ultaire AKP the lowest values of all investigated PAEK materials initially, after thermocycling and after autoclaving ($p < 0.001$). Microscopic examinations showed that artificial aging did not cause any major modifications of the materials.

Significance. Additively manufactured PEEK materials showed lower Martens parameters than milled ones, whereas horizontally printed specimens presented higher values than vertically printed ones. Artificial aging had a negative effect on the Martens parameters, but not on the surface topography.

* *Corresponding author.*
E-mail address: Alexander.Prechtel@med.uni-muenchen.de (A. Prechtel).
[1] Joint first authors.
https://doi.org/10.1016/j.dental.2019.11.017
0109-5641/

1. Introduction

In dentistry, the possibility of using additive manufacturing (AM) technologies for producing objects layer by layer has been used in a digital workflow with data acquisition, computer-aided design (CAD) and computer-aided manufacturing (CAM) since the late 1980s [1]. In recent years, the development of new materials, printing techniques and machines has increased rapidly, giving three-dimensional (3D) printing the potential to revolutionize traditional dentistry in clinical treatment, research and education. Its indications extend from prosthodontics, oral and maxillofacial surgery to orthodontics, endodontics and periodontics [2]. The advantages of AM are very convincing, such as the fabrication of complex individual geometries, on-demand production of small quantities, a high economic efficiency due to a theoretical material yield of 100 %, accelerated and cost-effective innovation processes, as well as high precision [3]. On the negative side, high process- and material costs, a complex workflow with presupposed technical know-how, anisotropic behaviour as well as a time-consuming postprocessing of the printed object have to be mentioned. 3D printing is already successfully applied in various medical and dental fields [4,5].

Several printing techniques are available for processing polymers such as polyamide (PA), polycarbonate (PC) and acrylonitrile-butadiene-styrene (ABS); namely: stereolithography (SLA), selective laser sintering (SLS), inkjet 3D printing (3DP) and fused layer manufacturing (FLM) [6]. The last one is suitable for thermoplastic elastomers (TPE) such as modern high-performance polymers from the group of polyaryletherketon (PAEK).

Especially, the increasing demand of many patients for biocompatible, metal-free and esthetic dentures makes PAEK attractive as an alternative to conventional restorative materials, where polyetheretherketon (PEEK) represents the best known and dominant member of the PAEK family.

PAEKs are semi-crystalline thermoplastics in which aromatics are linearly linked in different orders via ether and ketone connections [7]. The amount of these functional groups determines the mechanical and thermal properties. The synthesis is based on condensation polymerization using electrophilic or nucleophilic substitution. Due to its excellent biocompatibility [8,9] and its high mechanical properties, it has been used for many years in medicine for spinal implants, femoral stems or trauma implants [7,10]. For dentistry, the chemical stability, X-ray translucency, bone-like elastic modulus (3–4 GPa), tooth-like colour and a low plaque accumulation are very advantageous [7]. In contrast to conventional dental methylmethacrylate-based polymers, PAEKs are free of residual monomer, making them ideal as an alternative material not only for patients with a high risk of allergies. So far, only one case of a chronic systemic allergy to PEEK has been reported in the literature [11]. The application of PAEKs in dentistry has a wide range. For example, they are used as frameworks for crowns and bridges, dentures bases and clasps, partial crowns, implants, implant abutments and esthetic orthodontic wires [12–16].

PAEK polymers can be processed in a variety of ways. Since 2011 CAD/CAM-supported milling of industrially prefabricated blanks is available [17]. For processing PAEKs for 3D printing technology FLM is available, which was firstly reported by Valentan in 2013 [18]. In this technique, the solid filament is heated at the nozzle to a semi-liquid state and then placed on the printer's building platform or previously printed layers. The single layers are then fused together to the final component [6]. Due to the high crystalline melt transition temperature (T_m = 343 °C) of PEEK, a special 3D printer is required that can provide the high melt and ambient temperatures and keep the temperature of the nozzle, building platform and chamber constant for a long time in a controlled process. Previous literature about PEEK processed via FLM was based mostly on custom-made printing machines. It was found by fourier transform infrared (FTIR) spectroscopy analyses and in-vitro cytotoxicity tests that the high temperatures do not modify the molecular structure of PEEK and no toxic substances were produced during the printing process, which is very important for medical use [19]. Generally, the few existing studies have shown that the mechanical properties of printed components out of PEEK via FLM depend on printing temperature, layer thickness, printing speed, extrusion path, filling ratio, raster angle and printing direction [20–23].

However, data on the mechanical properties of FLM manufactured PEAK components for dental applications is still limited. The aim of this study was to examine the influence of artificial aging on the hardness of PEEK materials manufactured with either a commercially available FLM printer or different PAEK polymers milled from industrially prefabricated blanks.

Hardness is an important parameter for the durability of a material [24]. The Martens hardness test method is particularly suitable for polymer-based dental materials, in which the effects of elastic and plastic deformation are determined. Furthermore, this method of measurement is independent of the optical and subjective measurement of indentations of the indenter.

The null hypothesis was that there were no differences in the Martens parameters between 3D printed and milled PAEK materials regardless artificial aging and printing direction.

2. Materials and methods

A total number of 204 specimens (10 mm × 10 mm × 5 mm) were manufactured, embedded in acrylic resin (ScandiQuick A and B, ScanDia, Hagen, Germany, LOT No. 09201 and 09202) and polished with P500 for 30 s and with P1200 (SiC-Papier, Struers, Ballerup, Denmark) for 15 s with an half-automatic polishing machine (Tegramin-20, Struers) under permanent water cooling. Finally, the specimens were cleaned in an ultrasonic bath (L&R Transistor/ Ultrasonic T-14, L&R, Kearny, NJ, USA) for 5 min in distilled water. The study design is depicted in Fig. 1.

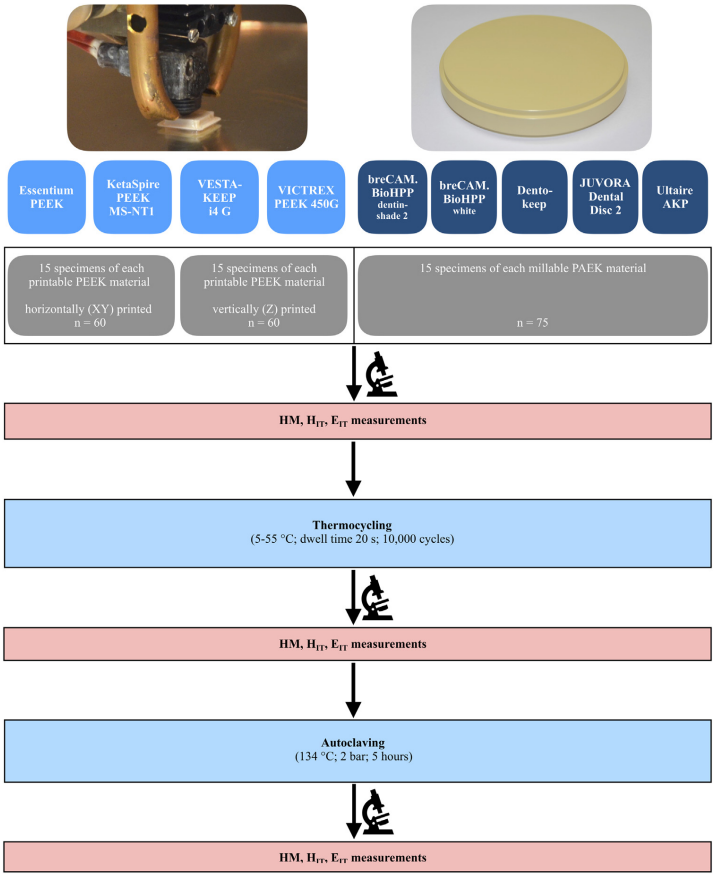

Fig. 1 – Study design: hardness measurements and microscopic examinations initially and after artificial aging on printed and milled specimens.

2.1. *3D printed PEEK specimens*

For each printable PEEK material (Essentium PEEK, KetaSpire PEEK MS-NT1, VICTREX PEEK 450G, VESTAKEEP i4 G) (Table 1) thirty specimens were manufactured as filament by FLM (filament diameter: 1.75 mm) using the printer HTRD1.1 (KUMOVIS GmbH, Munich, Germany). The technical specifications of the printer are shown in Table 2. In this 3D printer, the extruder moves along the X-, Y- and Z-axes, while the building platform remains in a fixed position. Before the printing process the filament was put into an oven (Heraeus RT 360, Heraeus Holding GmbH, Hanau, Germany) at 120 °C for 12 h to extract moisture from the material.

Initially, pilot prints (P1-P9) were made, whereby the influence of different printing speeds (600, 900 and 1200 mm/min), layer heights (0.10, 0.15, 0.20 and 0.30 mm) and extrusion widths (0.30, 0.40 and 0.50 mm) on the Martens parameters was investigated in order to subsequently determine the final printing parameters for the main prints. These were: printing speed 900 mm/min, layer height 0.2 mm and extrusion width 0.4 mm. The specimens of the pilot and main prints were all manufactured with 100 % interior fill.

In order to evaluate the influence of the printing direction (layer orientation) on the Martens parameters, fifteen specimens for each printable PEEK material were printed in either horizontal (XY) or vertical (Z) directions

(Fig. 2). With the horizontally printed specimens, the layers were oriented perpendicular to the measuring direction and for the vertical ones, the layer orientation was parallel to the penetration of the indenter pyramid.

After the printing process all specimens were carefully removed with a cutter from the building platform immedi-

Table 1 – Summery of production process, PAEK materials, abbreviations, compositions, manufacturer and LOT numbers.

Production process	PAEK material	Abbreviation	Composition	Manufacturer	LOT No.
Printing (horizontal and vertical direction)	Essentium PEEK	ESS	Polyetheretherketon, unfilled	Essentium Inc., Pflugerville, USA	1-80601
	KetaSpire® PEEK MS-NT1	KET	Polyetheretherketon, unfilled	Solvay Specialty Polymers USA, L.L.C., Alpharetta GA, USA	1850009004
	VESTAKEEP® i4 G (exp. material)	VES	Polyetheretherketon, unfilled	Evonik Industries AG, Essen, Germany	"testing grade" version
	VICTREX® PEEK 450G	VIC	Polyetheretherketon, unfilled	Victrex plc., Thornton Cleveleys, UK	7082
Milling	breCAM.BioHPP®	BHD	Polyetheretherketon, filled with app. 30 % TiO_2, dentin-shade 2	bredent, Senden, Germany	438245
		BHW	Polyetheretherketon, filled with app. 20 % TiO_2, white		406700
	Dentokeep	DEN	Polyetheretherketon, filled with app. 20 % TiO_2	Trading GmbH & Co. KG, Karlsruhe, Germany	11DK18001
	JUVORA™ Dental Disc 2	JUV	Polyetheretherketon, unfilled	JUVORA Ltd., Thornton Cleveleys, UK	WO000042IDML
	Ultaire™ AKP	ULT	Aryl-Keton-Polymer, unfilled	Solvay Dental 360™, Alpharetta GA, USA	1641125024032

Table 2 – Technical specifications of HTRD1.1.

Nozzle temperature	410 °C
Nozzle diameter	0.4 mm
Heated building chamber	200 °C
Heated building platform	250 °C
Ventilation	Heated laminar airflow
Clean room filter system	No
Slicing software	Simplify3D® (version 4.1, Cincinnati, OH, USA)

ately, cooled down at room temperature and measured 24 h later.

2.2. *Milled PAEK specimens*

For each millable PAEK material (breCAM.BioHPP, Dentokeep, JUVORA™ Dental Disc 2, Solvay Ultaire™ AKP) (Table 1) fifteen specimens were milled out of pre-fabricated blocks with a handpiece (KaVo EWL K9, KaVo Dental, Biberach/ Riß, Germany).

2.3. *Hydrothermal aging process of specimens*

The specimens were thermocycled (Thermocycler THE 1100, SD Mechatronics, Feldkirchen-Westerham, Germany) between 5 and 55 °C with a dwell time for 20 s for 10,000 cycles. Subsequently, the hydrothermal aging was performed using an autoclave for five hours at 134 °C and 2 bar (Euroklav 29-S, MELAG Medizintechnik oHG, Berlin, Germany).

2.4. *Martens hardness (HM), indentation hardness (H_{IT}) and indentation modulus (E_{IT})*

An universal hardness testing machine (ZHU 0.2/ Z2.5, Zwick Roell, Ulm, Germany) was used to determine the Martens parameters (HM in N/mm², H_{IT} in N/mm² and E_{IT} in kN/mm²) initially and directly after the thermocycling and autoclaving process. The measurement of Martens parameters is based on the principle of pressing an indenter into the surface of a specimen and continuously measuring the force F (in N) and the penetration depth h (in μm) during the loading and unloading phase (DIN EN ISO 14577) [25].

During measurement, the diamond indenter pyramid ($\alpha = 136°$) of the testing machine was pressed vertically into the surface of the specimen for 10 s with a load of 9.807 N. The maximum penetration depth of the pyramid into the material was 0.05 mm. The movement of the indenter represented the sum of elastic deformation of the surface together with the plastic penetration depth [24]. HM, H_{IT} and E_{IT} were automatically calculated with the corresponding software (testXpert V12.3 Master, Zwick Roell) using the following equations (DIN EN ISO 14577) [25]:

$$HM = \frac{F}{A_s(h)} = \frac{F}{26.43 \times h^2}$$

$$H_{IT} = \frac{F_{max}}{A_p}$$

$$E_{IT} = \left(1 - v_s^2\right) \times \left(\frac{1}{E_r} - \frac{\left(1 - v_i^2\right)}{E_i}\right)^{-1} \text{ with } E_r = \frac{\sqrt{\pi}}{2C\sqrt{A_p}}$$

with HM in N/mm², F (test force) in N, $A_s(h)$ (surface area of the indenter at distance h from the trip) in mm², h (inden-

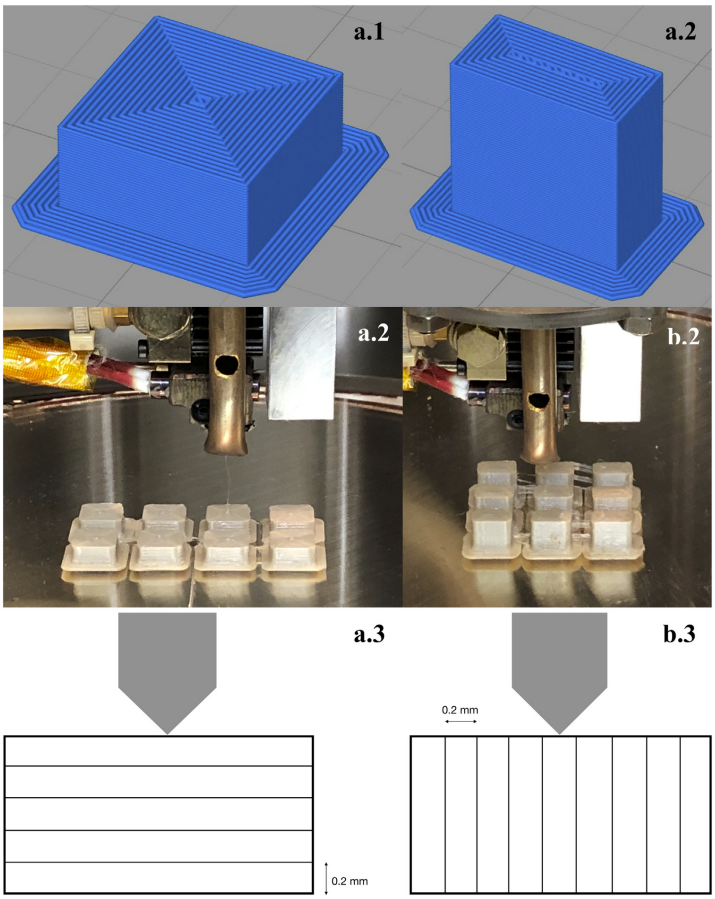

Fig. 2 – Sliced (1), printed (2) and measured (3) specimens in horizontal (a) and vertical direction (b). The arrow indicates the penetration direction of the indenter pyramid.

tation depth under applied test force) in mm, H_{IT} in N/mm^2, F_{max} (maximum test force) in N, A_p (projected (cross-sectional) area of contact between the indenter and the test piece determined from the force-displacement curve and a knowledge of the area function of the indenter) in mm^2, E_{IT} in kN/mm^2, E_r (reduced modulus of the indentation contact) in N/mm^2, E_i (elastic modulus of the indenter) in N/mm^2, C (compliance of the contact), v_s (Poisson's ratio of the test piece) = 0.35 [26] and v_i (Poisson's ratio of the indenter) = 0.3.

Load-displacement curves (Fig. 3) indicated the penetration depth of the indenter in relation to the test force and provide further information about the material behaviour. The area between the loading and unloading curve indicated the penetration work of the material, while the area below the loading curve represented the irreversible plastic deformation work in particular and the area below the unloading curve showed the elastic re-deformation work [27].

2.5. *Surface topography analysis*

The surface topography of the specimens was analysed with a light microscope (Leica DM2700 M, Leica Microsystems GmbH, Wetzlar, Germany) using magnifications of ×5 and ×20 with the LAS X software (version 3.4.2, Leica Microsystems GmbH). Care was taken with a marker line and measured adjustment of the stage from the microscope to ensure that the same point was always observed for each specimen after the aging process in order to be able to make comparable statements.

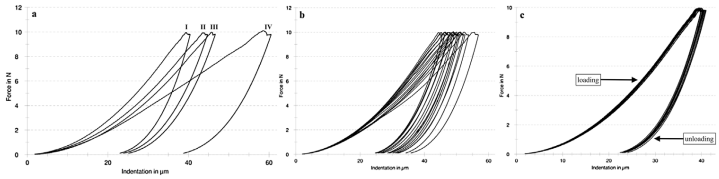

Fig. 3 – Load-displacement curves of BHD (a.I and c), ULT (a.II), horizontally printed ESS (a.III), vertically printed VIC (a.IV) and vertically printed KET (b).

2.6. *Statistical analysis*

All statistical analyses were performed with the SPSS statistics program (version 25.0.0.1, IBM, Armonk, NY, USA). Descriptive statistics were computed. The presumption of normal distribution was tested using Kolmogorov-Smirnov test. The univariate ANOVA with partial eta squared (η_p^2) was calculated for an overall consideration of the data. To determine significant differences between the various PAEK materials and printing direction non-parametric Kruskal–Wallis- and Mann–Whitney-U-Test were used. To evaluate the aging process Friedman- and Wilcoxon-Test were calculated. A value of $p < 0.05$ was considered as significant.

3. Results

The descriptive statistics are summarized in Tables 3 and 4. Data were analysed nonparametrically, because the Kolmogorov-Smirnov test showed that more than 5% of the tested groups (47/117) deviated from the normal distribution.

3.1. *Results of the pilot prints*

Analysing printing speed, specimens printed at 900 mm/min and 1200 mm/min showed the highest HM ($p = 0.290$) and E_{IT} values ($p = 0.170$). For H_{IT} all three examined printing speeds were within the same value range ($p = 0.070$). With regard to layer height, no differences could be found in the Martens parameters between the various settings (HM: $p = 0.626$; H_{IT}: $p = 0.547$; E_{IT}: $p = 0.562$). For extrusion width, specimens printed with 0.4 mm and 0.5 mm showed the highest HM ($p = 0.820$), E_{IT} ($p = 0.796$) and H_{IT} values ($p = 0.616$). Finally, differences in the Martens parameters between horizontally and vertically printed specimens were found (HM: $p = 0.001$; H_{IT}: $p = 0.002$; E_{IT}: $p < 0.001$).

3.2. *Results of the printed and milled PAEK specimens*

Regarding printed specimens the highest impact on HM and E_{IT} was exerted by material (HM: $\eta_p^2 = 0.387$, $p < 0.001$; E_{IT}: $\eta_p^2 = 0.405$, $p < 0.001$) followed by the printing direction (HM: $\eta_p^2 = 0.368$, $p < 0.001$; E_{IT}: $\eta_p^2 = 0.283$, $p < 0.001$) and the aging process (HM: $\eta_p^2 = 0.020$, $p = 0.036$; E_{IT}: $\eta_p^2 = 0.097$, $p < 0.001$). For H_{IT}, the printing direction had the highest impact ($\eta_p^2 = 0.374$, $p < 0.001$) followed by material ($\eta_p^2 = 0.361$, $p < 0.001$), while the aging process did not show an effect ($p = 0.387$). The binary combination (material and printing direction) was also significant (HM: $\eta_p^2 = 0.294$, $p < 0.001$; H_{IT}: $\eta_p^2 = 0.308$, $p < 0.001$; E_{IT}: $\eta_p^2 = 0.211$, $p < 0.001$).

For the milled specimens the highest impact was exerted by material (HM: $\eta_p^2 = 0.817$, $p < 0.001$; H_{IT}: $\eta_p^2 = 0.834$, $p < 0.001$; E_{IT}: $\eta_p^2 = 0.738$, $p < 0.001$) followed by the aging process (HM: $\eta_p^2 = 0.256$, $p < 0.001$; H_{IT}: $\eta_p^2 = 0.208$, $p < 0.001$; E_{IT}: $\eta_p^2 = 0.201$, $p < 0.001$) and the binary combination between both parameters (HM: $\eta_p^2 = 0.122$, $p < 0.001$; H_{IT}: $\eta_p^2 = 0.128$, $p < 0.001$; E_{IT}: $\eta_p^2 = 0.064$, $p < 0.001$).

In general, milled specimens showed higher values for the Martens parameters than printed ones ($p < 0.001$). Differences between the materials within one aging level ($p < 0.001$) have been recorded. Furthermore, horizontally printed specimens presented higher Martens parameters than vertical ones, regardless of material or aging process ($p < 0.001$).

Essentium PEEK (ESS) showed the highest and VICTREX PEEK 450 G (VIC) the lowest values of all printable PEEK materials initially, after thermocycling and after autoclaving ($p < 0.001$), whereby VIC showed initially a comparable HM value with VESTAKEEP i4 G (VES) ($p = 0.290$) and KetaSpire PEEK MS-NT1 (KET) ($p = 0.104$). For H_{IT} initially and after thermocycling, VIC was with KET ($p = 0.228$ and $p = 0.143$) and VES ($p = 0.340$ and $p = 0.301$) in the same value range. KET and VES showed comparable E_{IT} values initially ($p = 0.405$), HM ($p = 0.403$) and E_{IT} ($p = 0.603$) after thermocycling and HM ($p = 0.673$), H_{IT} ($p = 0.853$) and E_{IT} ($p = 0.246$) after autoclaving (Fig. 3).

For the milled specimens, breCAM.BioHPP with app. 30 % TiO_2 (BHD) presented initially, after thermocycling and after autoclaving the highest Martens parameters ($p < 0.001$). Ultaire AKP (ULT) showed initially and after the hydrothermal aging the lowest Martens parameters of all tested millable PAEK materials ($p < 0.001$) (Fig. 4).

Generally, there are significant differences in the Martens parameters due to the aging process, with the highest values being reached initially ($p < 0.001$). Dentokeep (DEN), horizontally printed KET, vertically printed VES and horizontally as well as vertically printed VIC showed within their group comparable Martens parameters independently of the aging process. Horizontally printed ESS and VES as well as vertically printed ESS and KET presented initially higher E_{IT} than after autoclaving ($p = 0.008$–0.046). Specimens printed vertically out of ESS showed after the hydrothermal aging significant lower HM and H_{IT} values than initially.

BHD and breCAM.BioHPP with app. 20 % TiO_2 (BHW) presented initially higher Martens parameters than after the aging process ($p < 0.001$). For JUVORA Dental Disc 2 (JUV)

Table 3 – Descriptive statistics for Martens parameters of the pilot prints according to the printing direction, printing speed, layer height, extrusion width and printing time.

Specimen	Printing direction	Printing speed [mm/min]	Layer height [mm]	Extrusion width [mm]	Printing time [min]	HM [N/mm²]			H_{IT} [N/mm²]			E_{IT} [kN/mm²]		
						Mean ± SD	95 % CI	Min/Median/Max	Mean ± SD	95 % CI	Min/Median/Max	Mean ± SD	95 % CI	Min/Median/Max
P1	horizontal	900	0.20	0.40	22	153 ± 21.9^{Bb}	129; 177	114/156/179	230 ± 39.4^{b}	187; 272	159/235/275	3.72 ± 0.256^{Bb}	3.43; 3.99	3.3/3.7/4.1
P2	horizontal	1200	0.20	0.40	9	131 ± 29.6^{ABb}	99; 163	87/134/171	196 ± 49.7^{b}	143; 249	123/198/266	3.20 ± 0.540^{ABb}	2.62; 3.77	2.4/3.4/3.8
P3	horizontal	600	0.20	0.40	33	98.5 ± 49.1^{Ab}	46; 150	40/92/163	145 ± 82.4^{b}	58.1; 232	49/133/251	2.73 ± 0.638^{Ab}	2.05; 3.41	2.0/2.5/3.7
P4	horizontal	900	0.20	0.30	22	93.8 ± 31.5^{Ba}	59; 127	66/87/153	140 ± 56.4^{a}	80.2; 199	94/123/248	2.38 ± 0.504^{Ba}	1.84; 2.92	1.9/2.3/3.2
P5	horizontal	900	0.20	0.50	22	142 ± 34.7^{Bb}	104; 178	98/146/185	212 ± 56.6^{b}	151; 272	142/218/281	3.45 ± 0.663^{Bb}	2.74; 4.15	2.6/3.6/4.4
P6	horizontal	900	0.30	0.40	13	157 ± 25.5^{1Bb}	129; 184	114/170/176	237 ± 43.0^{b}	190; 283	161/257/272	3.73 ± 0.472^{Bb}	3.22; 4.23	3.1/3.9/4.2
P7	horizontal	900	0.15	0.40	25	148 ± 27.1^{Bb}	118; 177	102/148/180	222 ± 44.9^{b}	174; 270	146/221/276	3.60 ± 0.566^{Bb}	2.99; 4.20	2.7/3.7/4.1
P8	horizontal	900	0.10	0.40	41	135 ± 42.4^{Bb}	89; 180	80/149/178	196 ± 70.5^{b}	120; 271	105/220/271	3.62 ± 0.611^{Bb}	2.96; 4.26	2.9/3.7/4.3
P9	vertical	900	0.20	0.40	43	181 ± 8.66^{Bb}	170; 190	170/183/190	270 ± 16.1^{b}	252; 287	250/273/287	4.42 ± 0.117^{Bb}	4.28; 4.54	4.2/4.5/4.5

^{A,B}Indicate significant differences among the printing speed.
^{a,b}Indicate significant differences among the extrusion width.
^{1} Indicates group without normal distribution.

Table 4 – Descriptive statistics for Martens parameters according to the production process, PAEK material and aging process.

Production process (Printing direction)	PAEK material	Aging process	HM [N/mm²]			HIT [N/mm²]			EIT [kN/mm²]		
			MW ± SD	95 % CI	Min/Median/ Max	MW ± SD	95 % CI	Min/Median/ Max	MW ± SD	95 % CI	Min/Median/ Max
Printing (horizontal)	ESS	Initial	185 ± 3.51^{B}	181; 187	179/185/191	277 ± 6.05^{B}	272; 281	267/277/287	4.46 ± 0.063^{1,Cb}	4.41; 4.50	4.4/4.5/4.6
		Thermocycling	179 ± 5.87 ^{C}	175; 183	165/179/188	270 ± 9.69^{B}	263; 275	245/ 271/282	4.31 ± 0.125^{Ca}	4.23; 4.39	4.1/4.3/4.5
		Autoclaving	181 ± 5.46^{C}	177; 185	171/184/188	273 ± 9.16^{C}	268; 278	252/276/282	4.34 ± 0.140^{1,Ca}	4.27; 4.42	4.0/4.4/4.5
Printing (vertical)		Initial	179 ± 14.5^{1,Bb}	169; 187	129/182/190	271 ± 25.9^{1,Bb}	255; 285	180/277/286	4.25 ± 0.226^{1,Cb}	4,11; 4,38	3.7/4.3/4.6
		Thermocycling	166 ± 26.8^{1,Ca}	150; 182	89/175/189	249 ± 45.8^{1,Ba}	222; 275	119/267/284	4.08 ± 0.402^{Cab}	3.84; 4.31	3.0/4.2/4.5
		Autoclaving	169 ± 10.0^{Ca}	161; 175	150/168/183	262 ± 15.4^{Ca}	252; 271	225/264/279	3.86 ± 0.412^{1,Ca}	3.62; 4.09	3.2/4.0/4.3
Printing (horizontal)	KET	Initial	171 ± 33.2^{1,A}	151; 189	74/182/189	257 ± 52.6^{1,A}	226; 287	105/275/285	4.09 ± 0.685^{1,B}	3.69; 4.47	2.1/4.3/4.5
		Thermocycling	177 ± 16.0^{1,B}	166; 186	137/181/192	268 ± 20.4^{1,A}	255; 280	216/273/291	4.14 ± 0.488^{1,B}	3.86; 4.42	3.0/4.3/4.5
		Autoclaving	164 ± 20.9^{B}	151; 176	114/159/187	250 ± 31.3^{B}	231; 268	171/255/283	3.81 ± 0.553^{B}	3.49; 4.12	2.8/3.9/4.5
Printing (vertical)		Initial	150 ± 17.8^{A}	139; 160	115/147/178	220 ± 32.5^{A}	201; 239	160/215/269	3.83 ± 0.226^{Bb}	3.69; 3.96	3.3/3.8/4.3
		Thermocycling	153 ± 21.4^{B}	140; 166	107/155/184	226 ± 35.6^{A}	204; 246	153/227/281	3.87 ± 0.392^{Bb}	3.63; 4.09	2.9/3.9/4.4
		Autoclaving	144 ± 28.4^{B}	127; 160	86/142/177	217 ± 46.9^{B}	190; 244	120/208/273	3.45 ± 0.576^{1,Ba}	3.12; 3.78	2.1/3.6/4.1
Printing (horizontal)	VES	Initial	168 ± 10.4^{A}	160; 174	141/171/180	252 ± 17.5^{A}	240; 262	204/259/270	4.07 ± 0.231^{1,Bb}	3.93; 4.21	3.7/4.2/4.4
		Thermocycling	172 ± 10.7^{1,A}	164; 178	142/176/180	258 ± 17.1^{1,A}	247; 268	208/265/271	4.12 ± 0.265^{1,Bb}	3.96; 4.27	3.6/4.2/4.4
		Autoclaving	161 ± 16.5^{B}	151; 171	113/169/179	246 ± 26.0^{1,B}	231; 261	161/254/268	3.78 ± 0.420^{1,Ba}	3.53; 4.02	3.1/4.0/4.3
Printing (vertical)		Initial	153 ± 19.1^{A}	141; 164	113/157/176	225 ± 33.2^{A}	205; 244	157/235/264	3.87 ± 0.269^{B}	3.70; 4.02	3.3/3.9/4.3
		Thermocycling	160 ± 14.7^{A}	150; 169	130/165/176	237 ± 26.0^{A}	221; 251	183/246/266	3.97 ± 0.212^{B}	3.84; 4.10	3.6/4.0/4.3
		Autoclaving	156 ± 13.0^{B}	148; 164	133/158/176	234 ± 22.9^{B}	220; 247	188/234/265	3.80 ± 0.254^{B}	3.65; 3.95	3.2/3.8/4.2
Printing (horizontal)	VIC	Initial	176 ± 20.0^{1,A}	163; 187	122/182/190	268 ± 33.8^{1,A}	247; 287	175/279/291	4.01 ± 0.378^{A}	3.86; 4.30	3.2/4.2/4.5
		Thermocycling	176 ± 16.6^{1,A}	165; 186	129/181/189	270 ± 27.2^{1,A}	253; 285	190/281/288	4.05 ± 0.346^{1,A}	3.85; 4.25	3.3/4.2/4.4
		Autoclaving	159 ± 32.8^{A}	140; 178	101/171/196	244 ± 54.7^{A}	212; 275	141/266/314	3.67 ± 0.610^{A}	3.32; 4.02	2.8/3.8/4.3
Printing (vertical)		Initial	102 ± 13.8^{A}	94.1; 110	78/101/127	144 ± 23.6^{A}	129; 157	105/143/189	2.91 ± 0.183^{A}	2.79; 3.01	2.6/2.9/3.2
		Thermocycling	104 ± 13.1^{A}	97.0; 112	77/103/131	149 ± 23.1^{A}	135; 162	103/143/199	2.90 ± 0.156^{A}	2.80; 2.99	2.6/2.9/3.1
		Autoclaving	108 ± 13.4^{A}	99; 115	90/105/132	156 ± 23.7^{A}	142; 170	126/152/203	2.83 ± 0.231^{A}	2.68; 2.96	2.4/2.8/3.2
	BHD	Initial	227 ± 3.58^{Fe}	224; 230	221/227/233	329 ± 5.85^{Fe}	324; 332	318/329/338	5.98 ± 0.108^{1,Ge}	5.91; 6.05	5.8/6.0/6.1
		Thermocycling	222 ± 7.73^{Gd}	216; 227	204/223/231	322 ± 13.0^{1,Ed}	313; 330	287/326/335	5.84 ± 0.184^{Gd}	5.72; 5.95	5.6/5.9/6.1
		Autoclaving	205 ± 18.2^{Gc}	194; 216	155/208/224	303 ± 12.1^{Ec}	296; 311	276/302/321	5.29 ± 0.944^{1,Gc}	4.77; 5.81	2.6/5.6/6.1
	BHW	Initial	220 ± 3.31^{Ee}	216; 222	215/220/228	322 ± 5.01^{Ed}	318; 325	315/321/335	5.59 ± 0.110^{Fe}	5.52; 5.66	5.4/5.6/5.8
		Thermocycling	219 ± 5.84^{Fd}	214; 223	205/219/227	322 ± 7.72^{Ee}	316; 327	307/322/332	5.56 ± 0.196^{Fd}	5.44; 5.67	5.0/5.6/5.8
		Autoclaving	201 ± 12.7^{Ec}	192; 208	172/203/220	297 ± 14.6^{Ec}	287; 306	268/298/321	5.00 ± 0.529^{Fc}	4.69; 5.30	3.8/5.1/5.7
Milling	DEN	Initial	217 ± 10.8^{1,E}	210; 224	199/222/228	317 ± 18.6^{1,E}	305; 327	282/324/336	5.61 ± 0.210^{F}	5.48; 5.74	5.2/5.7/5.8
		Thermocycling	217 ± 11.2^{1,F}	209; 223	190/222/229	317 ± 19.2^{1,E}	305; 328	277/325/337	5.57 ± 0.244^{1,F}	5.42; 5.71	4.9/5.6/5.8
		Autoclaving	212 ± 13.6^{1,G}	203; 220	169/212/228	314 ± 8.22^{F}	308; 319	301/311/332	5.31 ± 0.735^{1,G}	4.89; 5.73	2.9/5.5/5.9
	JUV	Initial	217 ± 5.96^{Ed}	212; 220	204/217/225	330 ± 11.8^{1,F}	322; 337	304/332/344	5.06 ± 0.074^{1,Ed}	5.00; 5.11	4.9/5.1/5.2
		Thermocycling	215 ± 7.00^{1,Ed}	209; 219	202/217/223	327 ± 13.7^{1,F}	318; 328	301/333/342	5.01 ± 0.099^{1,Ed}	4.94; 5.07	4.8/5.0/5.2
		Autoclaving	208 ± 8.48^{Fc}	202; 213	188/210/222	320 ± 16.0^{1,G}	310; 329	285/322/360	4.77 ± 0.215^{Ec}	4.64; 4.90	4.4/4.7/5.1
	ULT	Initial	171 ± 3.68^{1,Dd}	167; 174	160/172/175	257 ± 7.37^{1,D}	252; 262	235/259/264	4.10 ± 0.054^{1,Dd}	4.06; 4.14	4.0/4.1/4.2
		Thermocycling	168 ± 4.73^{Dc}	164; 171	156/169/176	253 ± 9.24 ^{D}	247; 259	232/254/267	4.05 ± 0.074^{1,Dcd}	3.99; 4.09	3.9/4.0/4.2
		Autoclaving	166 ± 4.17^{Dc}	162; 169	156/167/171	251 ± 4.56^{D}	247; 254	239/251/258	3.95 ± 0.192^{1,Dc}	3.83; 4.06	3.3/4.0/4.1

$^{A–G}$Indicate significant differences among all tested materials within one Martens parameter and one aging process.
$^{a–f}$Indicate significant differences among the aging process within one Martens parameter and one material.
^{1} Indicates groups without normal distribution.

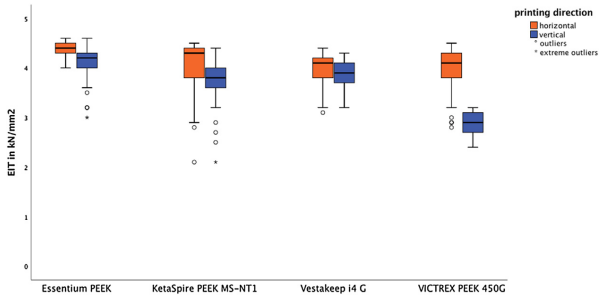

Fig. 4 – Boxplot of E_{IT} of the printed PEEK materials in relation to the printing direction regardless of the aging process.

and ULT, the values for HM ($p = 0.008$ and $p = 0.002$) and E_{IT} ($p = 0.001$ and $p = 0.003$) are initially higher than after autoclaving, whereas for JUV no difference between the initial and aged values (HM: $p = 0.509$; E_{IT}: $p = 0.131$) and for ULT no difference between after thermocycling and after autoclaving (HM: $p = 0.147$; E_{IT}: $p = 0.058$) was observed.

Considering the load-displacement curves the loading and unloading curve of BHD had the steepest gradients and the smallest area within the graph compared to the other materials, which means that less penetration work has been performed, which in turn indicated higher Martens parameters (Fig. 5a.I). With the vertically printed VIC, due to the flat gradient and the large area within the graph, a lot of penetration work was done so that the Martens parameters were lowest (Fig. 5a.IV).

The load-displacements curves of vertically printed KET (Fig. 5b) impressed with many slightly different curves, while the single curves of the specimens milled out of BHD overlapped and were nearly uniform (Fig. 5c).

3.3. *Surface topography analysis*

It could be observed microscopically that the hydrothermal aging did not cause any major modifications in all investigated PAEK materials. No cracks, fractures, voids and dimension changes could be detected, which occurred in the process of artificial aging (Fig. 6).

The printed specimens impressed with a high amount of artefacts such as not seamlessly placed extrusion paths, voids and air inclusions, which were already initially present directly after the printing process (Fig. 7).

4. Discussion

In this in-vitro investigation the effect of artificial aging on the Martens parameters to different 3D printed and milled PAEK materials was evaluated. Based on the results, the null hypotheses were rejected because differences between the printed and milled materials were found, the printing direction had a major influence and the aging process showed a negative effect on the Martens parameters.

In general, the Martens hardness test method is very well suited to investigate the elastic and plastic deformation of polymer-based materials like PAEK. The effects of morphological surface degradations on the mechanical properties caused by artificial aging can also be efficiently determined with this test method [28]. HM is different from H_{IT} only in the definition of the surface and indentation depth, so that there is a close relationship between both parameters [29]. H_{IT} examines the plastic behaviour of the material, while E_{IT} describes the elastic performance and is comparable with the Young's modulus [25].

Pilot prints were performed to determine suitable parameters for printing speed, layer height and extrusion width for the main prints. Regarding printing speed, 900 mm/min and 1200 mm/min showed comparable HM and E_{IT} values, but due to a subjectively higher printing quality of the specimens, the main prints were set to 900 mm/min. With the layer height no differences were found between the various settings on the Martens parameters. Consequently a good compromise between printing quality and printing time was found for 0.2 mm. The extrusion width was adjusted to 0.4 mm since it was the same size as the nozzle.

The differences observed between the printed and milled PAEK materials need to be highlighted. Milled specimens showed higher Martens parameters than printed ones. This fact might be explained by the standardized conditions of manufacturing by which a controlled crystallization process of the thermoplastic material can take place. With the printed specimens, the filament was melted in the extruder and subjected to a more or less controlled crystallization after the printing process, which can be influenced by many factors.

One important factor is temperature management and cooling procedures. In the present investigation, the printed specimens were all removed from the building platform immediately after the end of the printing process and cooled down slowly at room temperature. This raises the question of how the mechanical properties will behave if the component remained in the heated building chamber for an extended period of time or quickly cold down abruptly. As PAEK materials are polymers with a low degree of crystallization, their mechanical properties dependent on crystallinity [30]. It is to be expected that components will have better mechanical properties during post heat treatment, since the material

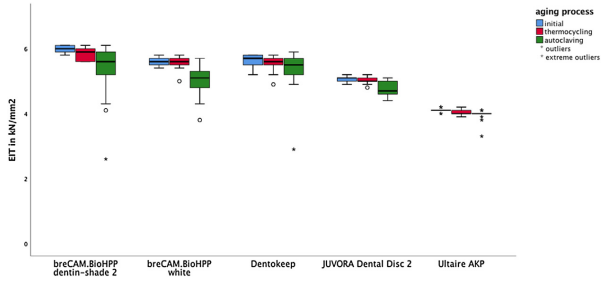

Fig. 5 – Boxplots of E_{IT} of the milled PAEK materials in relation to the aging process.

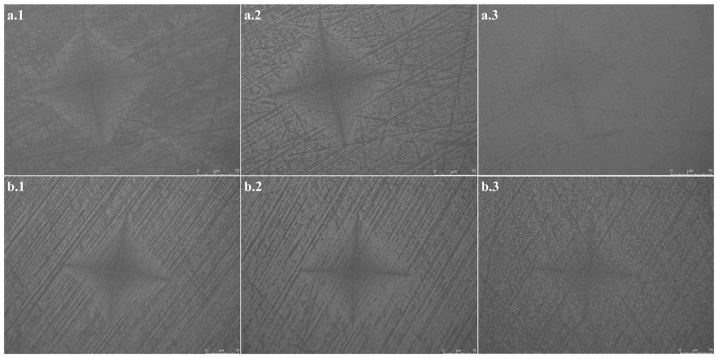

Fig. 6 – Microscope images (×20) with indentation of milled specimen out of BHD (a) and vertically printed ESS (b) initially (1), after thermocycling (2) and after autoclaving (3).

can crystallize even further after the printing process and cold crystallization can be prevented [23]. If cooling is too fast a lower degree of crystallization and cracks are possible due to a strong temperature change [31]. However, Valentan et al. have found that tensile strength decreases if the component is left at a high temperature in the building chamber for 12 h. Consequently, it should be removed from the printer immediately after the end of the printing process in order to achieve the best mechanical properties through slow cooling as performed in this study [18].

A further reason for the lower values of the printed specimens might be due to the artefacts such as voids and air inclusions within the printed specimen, which weakened the components mechanically. These artefacts are an indication of the presence of moisture in the filament [18]. The filament did not retain its dried state during the long printing process. It can be expected that it regained moisture from the ambient air. Therefore, a printer with a sealed chamber for the filament spool would be necessary to maintain a dried state from the oven during the printing process.

ESS showed the highest Martens parameters regardless of the aging process and printing direction, while VIC presented the lowest values. It is difficult to find an explanation for this. Unfortunately, the manufacturers do not provide much information about the materials' compositions, except that both materials have no integrated fillers. VIC is a material developed and optimized mainly for traditional injection molding. The experience gained a weaker adhesion between the single layers, which might explain why vertically printed VIC showed the lowest values.

In general, horizontally printed specimens showed higher values than vertical ones regardless of material and aging process. In case of the vertically printed specimens, the intender pyramid was pressed into the surface parallel to the layers, so that measurements were also made randomly at exactly the junction between two layers. Minimal tensile stresses were generated, which resulted in separation and sliding of two adjacent layers [32]. With the horizontal specimens, however, the pyramid penetrated into the material perpendicular to the layers, so that due to the small size of the pyramid only within one layer was measured and no tensile stresses were induced. The cohesive bonding within the same layer is also higher than the adhesive bonding between superimposed layers [33]. Rinaldi et al. observed in tensile tests that specimens printed in XY direction with 100% infill had better mechanical

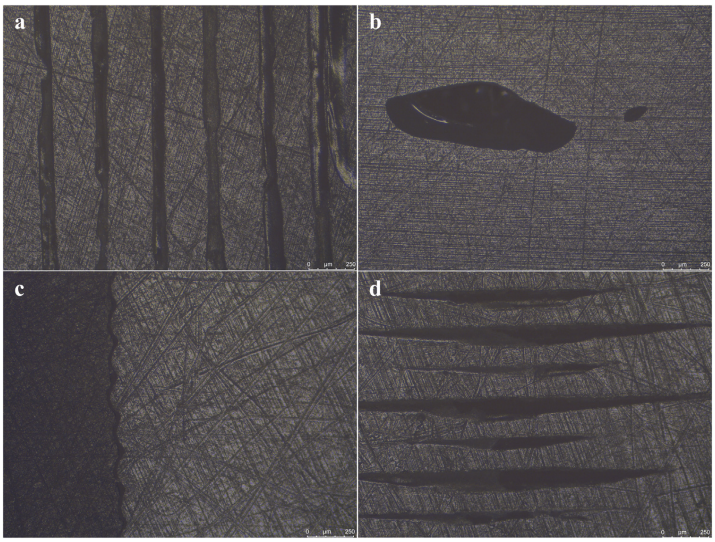

Fig. 7 – Microscope images (×5) of printed specimens with extrusion paths that were not seamlessly placed against each other (a), voids (b), wavy rim (c) and air inclusions between the layers (d).

properties than specimens printed in Z direction which is in accordance to our study [23].

The load-displacement curves of the printed materials impressed by a high variance of the curves, which indicated divergent penetration work and Martens parameters between the single specimens of the same material. An explanation might be that, although exactly the same printing parameters were set before each printing process, there were minimal different conditions for each print, such as room temperature, humidity, manually set Z-height of the extruder and sometimes a replacement of the extruder or the glass plate.

In order to compare the Martens parameters between all printable PEEK materials, each material was printed with exactly the same printing parameters. However, it would probably be necessary to find out the individual printing parameters for each material in order to achieve the best processing conditions and mechanical properties.

For the milled specimens, BHD showed the highest Martens parameters independently of the aging process. This material is filled with approximately 30 % titanium dioxide (TiO_2), which might explain these results. By adding TiO_2, aluminium trioxide (Al_2O_3), silicium dioxide (SiO_2) or carbon fibers, PAEK materials can be reinforced, which increases their mechanical properties [34,35]. BHW and DEN only contain approximately 20 % TiO_2 which might negatively have influenced the Martens parameters. However, esthetic properties usually suffer as a result of the additives, so that not all PAEK compounds can be used for aesthetic dental restorations in spite of better mechanical performance. ULT showed the lowest Martens parameters. This might be explained by the fact that this material is an unfilled aryl ketone polymer; but otherwise no further information about the chemical composition and exact filler content is available from the manufacturer.

When comparing Martens parameters with other dental CAD/CAM restorative materials, ceramics have by far the highest and PMMA-based composite materials the lowest values [27]. The investigated PAEK materials of the present study showed slightly better values than PMMA-based composite materials.

In dentistry, it is very important to use long-term restorative materials with a high clinical performance, as they are always exposed to a humid environment and dynamic temperature changes when taking food, liquids and breathing. For this reason, thermocycling and autoclaving were used in the present investigation, aiming to imitate artificial aging of the specimens. Thermocycling is often used in in-vitro studies, but there is no standardized protocol for number of cycles, dwell time and temperatures [36]. For this study 10,000 cycles were chosen, which corresponds to one year in-vivo situation, and temperatures of 5–55 °C, which are closest to the clinical situation. Autoclaving was performed at 134 °C, 2 bar and 5 h, which represents 15–20 years in-vivo situation [37].

Generally, temperature changes and thermal stresses lead to contraction and expansion in solid materials [36]. However, no cracks, fractures, voids and dimension changes could be observed under the light microscope. Further examinations using scanning electron microscopy are necessary to be able to show morphological changes caused by the aging process more precisely and to explain why the materials presented lower Martens parameter after the hydrothermal aging.

The aging process in this investigation has shown that horizontally printed ESS and VES, vertically printed ESS and KET,

BHD, BHW, JUV and ULT were quite vulnerable to aging processes, as illustrated by a decrease in Martens parameters. Due to possible microcracks caused by thermal stresses, moisture could be absorbed into the materials at the high temperature of the autoclave, so the mechanics suffers [38]. Most interestingly, the printable materials seemed to be more resistant to hydrothermal influences than milled ones, which is illustrated by a low $\eta_p{}^2$. It can be speculated that the moisture absorption capacity of PEEK filaments is lower than that of PEEK blanks, but this cannot be verified due to a lack of information from the manufacturers. In comparison to other materials such as hybrid materials, nanohybrid composites and PMMA-based materials, PEEK has the lowest water absorption [39].

For future research, thermodynamic and scanning electron microscopy investigations of the PEEK filaments are required, which can explain the different mechanical behaviour. In addition, the used FLM printer and most of the PEEK filaments have to be classified according to the Medical Devices Law in order to be able to use printed components in dentistry and to carry out in-vivo studies.

5. Conclusions

Within the limitations of this in-vitro study, it can be summarized that:

- PEEK specimens printed via FLM showed lower Martens parameters than milled ones, whereby printed ESS and milled BHD showed the highest values within their groups, independently of artificial aging.
- The printing direction showed an influence on the Martens parameters, whereas horizontally printed specimens had higher values than the vertical ones.
- PAEK compounds with TiO_2 resulted in higher Martens parameters than unfilled materials.
- The hydrothermal aging process showed a negative impact on the Martens parameters especially for the milled specimens; the printed specimens were more resistant to hydrothermal stresses.
- Additive manufacturing of PEEK for dental applications seems promising, but still needs further investigation to understand material and process influences better. Filament material filled with TiO_2 as well as application-oriented testing for specific use-cases should be looked at more closely in future.

Acknowledgements

The authors would like to thank KUMOVIS for providing the 3D printer HTRD1.1 and the PEEK filaments.

REFERENCES

[1] van Noort R. The future of dental devices is digital. Dent Mater 2012;28:3–12.
[2] Oberoi G, Nitsch S, Edelmayer M, Janjić K, Müller AS, Agis H. 3D printing — encompassing the facets of dentistry. Front Bioeng Biotechnol 2018:6.
[3] Ngo TD, Kashani A, Imbalzano G, Nguyen KTQ, Hui D. Additive manufacturing (3D printing): a review of materials, methods, applications and challenges. Compos B Eng 2018;143:172–96.
[4] Liaw C-Y, Guvendiren M. Current and emerging applications of 3D printing in medicine. Biofabrication 2017;9:024102.
[5] Tack P, Victor J, Gemmel P, Annemans L. 3D-printing techniques in a medical setting: a systematic literature review. Biomed Eng Online 2016;15:115.
[6] Wang X, Jiang M, Zhou Z, Gou J, Hui D. 3D printing of polymer matrix composites: a review and prospective. Compos B Eng 2017;110:442–58.
[7] Kurtz SM, Devine JN. PEEK biomaterials in trauma, orthopedic, and spinal implants. Biomaterials 2007;28:4845–69.
[8] Katzer A, Marquardt H, Westendorf J, Wening JV, von Foerster G. Polyetheretherketone — cytotoxicity and mutagenicity in vitro. Biomaterials 2002;23:1749–59.
[9] Poulsson AH, Eglin D, Zeiter S, Camenisch K, Sprecher C, Agarwal Y, et al. Osseointegration of machined, injection moulded and oxygen plasma modified PEEK implants in a sheep model. Biomaterials 2014;35:3717–28.
[10] Toth JM, Wang M, Estes BT, Scifert JL, Seim HB, Turner AS. Polyetheretherketone as a biomaterial for spinal applications. Biomaterials 2006;27:324–34.
[11] Maldonado-Naranjo AL, Healy AT, Kalfas IH. Polyetheretherketone (PEEK) intervertebral cage as a cause of chronic systemic allergy: a case report. Spine J 2015;15:e1–3.
[12] Zoidis P, Bakiri E, Polyzois G. Using modified polyetheretherketone (PEEK) as an alternative material for endocrown restorations: a short-term clinical report. J Prosthet Dent 2017;117:335–9.
[13] Tekin S, Cangül S, Adıgüzel Ö, Değer Y. Areas for use of PEEK material in dentistry. Int Dent Res 2018;8(2):84–92.
[14] Park C, Jun DJ, Park SW, Lim HP. Use of polyaryletherketone (PAEK) based polymer for implant-supported telescopic overdenture: a case report. J Adv Prosthodont 2017;9:74–6.
[15] Ali MZ, Baker S, Martin N. Traditional CoCr versus milled PEEK framework removable partial dentures–pilot randomised crossover controlled trial; interim findings. ConsEuro 2015. BM09 London.
[16] Schwitalla A, Müller WD. PEEK dental implants: a review of the literature. J Oral Implantol 2013;39:743–9.
[17] Stawarczyk B, Eichberger M, Uhrenbacher J, Wimmer T, Edelhoff D, Schmidlin PR. Three-unit reinforced polyetheretherketone composite FDPs: influence of fabrication method on load-bearing capacity and failure types. Dent Mater J 2015;34:7–12.
[18] Valentan B, Kadivnik Z, Brajlih T, Anderson A, Igor D. Processing poly(ether etherketone) on a 3d printer for thermoplastic modelling. Mater Tehnol 2013;47:715–21.
[19] Zhao F, Li D, Jin Z. Preliminary investigation of poly-ether-Ether-Ketone based on fused deposition modeling for medical applications. Materials 2018;11.
[20] Deng X, Zeng Z, Peng B, Yan S, Ke W. Mechanical properties optimization of poly-ether-Ether-Ketone via fused deposition modeling. Materials 2018;11.
[21] Yang C, Tian X, Li D, Cao Y, Zhao F, Shi C. Influence of thermal processing conditions in 3D printing on the crystallinity and mechanical properties of PEEK material. J Mater Process Technol 2017;248:1–7.
[22] Wu W, Geng P, Li G, Zhao D, Zhang H, Zhao J. Influence of layer thickness and raster angle on the mechanical properties of 3D-Printed PEEK and a comparative mechanical study between PEEK and ABS. Materials 2015;8:5834–46.
[23] Rinaldi M, Ghidini T, Cecchini F, Brandao A, Nanni F. Additive layer manufacturing of poly (ether ether ketone) via FDM. Compos B Eng 2018;145:162–72.

[24] Shahdad SA, McCabe JF, Bull S, Rusby S, Wassell RW. Hardness measured with traditional Vickers and Martens hardness methods. Dent Mater 2007;23:1079–85.
[25] BS EN ISO 14577-1:2002(E): Metallic materials — Instrumented indentation test for hardness and materials parameters — part 1: Test method.77.040.10.
[26] Greaves GN, Greer AL, Lakes RS, Rouxel T. Poisson's ratio and modern materials. Nat Mater 2011;10:823–37.
[27] Hampe R, Lümkemann N, Sener B, Stawarczyk B. The effect of artificial aging on Martens hardness and indentation modulus of different dental CAD/CAM restorative materials. J Mech Behav Biomed Mater 2018;86:191–8.
[28] Bürgin S, Rohr N, Fischer J. Assessing degradation of composite resin cements during artificial aging by Martens hardness. Head Face Med 2017;13:9.
[29] Ullner C. Die reihe DIN EN ISO 14577 — erste weltweit akzeptierte normen für die instrumentierte Eindringprüfung. Bundesanstalt für Materialforschung
[30] Yang X, Wu Y, Wei K, Fang W, Sun H. Non-isothermal crystallization kinetics of short glass Fiber reinforced poly (Ether ether ketone) composites. Materials 2018;11: 2094.
[31] Seo Y, Kim S. Nonisothermal crystallization behavior of poly(aryl ether ether ketone). Polym Eng Sci 2001;41:940–5.
[32] Alharbi N, Osman R, Wismeijer D. Effects of build direction on the mechanical properties of 3D-printed complete coverage interim dental restorations. J Prosthet Dent 2016;115:760–7.
[33] Puebla K, Arcaute K, Quintana R, Wicker RB. Effects of environmental conditions, aging, and build orientations on the mechanical properties of ASTM type I specimens manufactured via stereolithography. Rapid Prototyp J 2012;18:374–88.
[34] Panayotov IV, Orti V, Cuisinier F, Yachouh J. Polyetheretherketone (PEEK) for medical applications. J Mater Sci Mater Med 2016;27:118.
[35] Han X, Yang D, Yang C, Spintzyk S, Scheideler L, Li P, et al. Carbon Fiber reinforced PEEK composites based on 3D-Printing technology for orthopedic and dental applications. J Clin Med 2019;8:240.
[36] Morresi AL, D'Amario M, Capogreco M, Gatto R, Marzo G, D'Arcangelo C, et al. Thermal cycling for restorative materials: does a standardized protocol exist in laboratory testing? A literature review. J Mech Behav Biomed Mater 2014;29:295–308.
[37] Chevalier J. What future for zirconia as a biomaterial? Biomaterials 2006;27:535–43.
[38] Kumar A, Yap WT, Foo SL, Lee TK. Effects of sterilization cycles on PEEK for medical device application. Bioengineering 2018;5.
[39] Liebermann A, Wimmer T, Schmidlin PR, Scherer H, Loffler P, Roos M, et al. Physicomechanical characterization of polyetheretherketone and current esthetic dental CAD/CAM polymers after aging in different storage media. J Prosthet Dent 2016;115, 321-8.e2.

3.2 Originalarbeit: Prechtel A, Stawarczyk B, Hickel R, Edelhoff D, Reymus M. Fracture load of 3D printed PEEK inlays compared with milled ones, direct resin composite fillings, and sound teeth. Clin Oral Investig 2020; [epub 27.01.2020] (https://doi.org/10.1007/s00784-020-03216-5) IF 2018: 2.453

Zusammenfassung

Ziel: In dieser Untersuchung wurden die Bruchlasten, die Bruchbilder und der Einfluss einer Kausimulation von natürlichen Zähnen untersucht, die mit unterschiedlich verarbeiteten Restaurationsmaterialien versorgt waren. Es wurden 3D-gedruckte indirekte PEEK Inlays, gefräste indirekte PEEK Inlays, direkte Komposit-Füllungen und nicht restaurierte Zähne miteinander verglichen.

Material und Methode: Insgesamt wurden 112 Molaren mit standardisierten Klasse-I-Kavitäten auf folgende Weise mit Restaurationen versorgt (n = 16/ Gruppe): 3D-gedruckte indirekte PEEK Inlays mittels FLM Technologie aus den Materialien (1) ESS, (2) KET, (3) VES, (4) VIC; (5) gefräste indirekte PEEK Inlays aus JUV und (6) direkte Komposit-Füllungen aus Tetric EvoCeram (TET). Nicht restaurierte Zähne (7) dienten als positive Kontrollgruppe. Die Hälfte der Molaren aus jeder Gruppe (n = 8) wurde einer Kausimulation mit kombiniertem Thermolastwechsel ausgesetzt (1,2 Millionen x 50 N; 12.000 x 5 °C/ 55 °C). Anschließend wurden die Bruchlasten und die Bruchbilder von allen Zähnen ermittelt. Die statistische Auswertung der gewonnenen Daten erfolgte mittels Kolmogorov-Smirnov Test, zweifaktorieller Varianzanalyse mit partiellem Eta-Quadrat (η_p^2) und anschließendem post-hoc Scheffé Test sowie mittels Chi-Quadrat-Test ($p<0,05$). Außerdem wurden Weibull-Module m mit 95 % Konfidenzintervall berechnet.

Ergebnisse: ESS und TET zeigten die geringste Bruchlast von 956 N, wobei die nicht restaurierten Zähne die höchsten Werte von bis zu 2.981 N aufwiesen. Die Kausimulation hatte dabei keinen Einfluss ($p=0,132$). In Anbetracht der Weibull-Module präsentierte KET unter den Gruppen mit Kausimulation einen geringeren Wert als JUV, während TET unter den Gruppen ohne Kausimulation

die höchsten Werte lieferte. Alle indirekten Restaurationen zeigten Zahnfrakturen (75-100 %). Demgegenüber wiesen die direkten Komposit-Füllungen Frakturen des Restaurationsmaterials (87,5 %) und die gesunden Molaren zu 50 % komplette Zahnfrakturen sowie Höckerfrakturen auf.

Schlussfolgerung: Sowohl alle 3D-gedruckten und gefrästen indirekten PEEK Inlays als auch die direkten Komposit-Füllungen hielten den zu erwartenden physiologischen und maximal auftretenden Kaukräften stand.

Klinische Relevanz: Der 3D-Druck in der FLM Technologie von Inlays aus PEEK lieferte vielversprechende Ergebnisse in Bezug auf die mechanischen Eigenschaften. Jedoch sind Verbesserungen bezüglich der Druckgenauigkeit und der Ästhetik erforderlich, um damit als ein alternatives Material und Herstellungsverfahren in der Zahnmedizin erfolgreich zu sein.

Clinical Oral Investigations
https://doi.org/10.1007/s00784-020-03216-5

ORIGINAL ARTICLE

Fracture load of 3D printed PEEK inlays compared with milled ones, direct resin composite fillings, and sound teeth

Alexander Prechtel[1] · Bogna Stawarczyk[1] · Reinhard Hickel[2] · Daniel Edelhoff[1] · Marcel Reymus[2]

Received: 3 September 2019 / Accepted: 17 January 2020

Abstract

Objective The objective of this in vitro study was to investigate fracture load, fracture types, and impact of chewing simulation of human molars restored with 3D printed indirect polyetheretherketone (PEEK) inlays and compare these with milled indirect PEEK inlays, direct resin composite fillings, and sound teeth.

Materials and methods A total of 112 molars with form congruent class I cavities were restored with ($n = 16$/group) 3D printed indirect PEEK inlays via fused layer manufacturing (FLM): (1) Essentium PEEK (ESS), (2) KetaSpire PEEK MS-NT1 (KET), (3) VESTAKEEP i4 G (VES), (4) VICTREX PEEK 450G (VIC), (5) milled indirect PEEK inlays JUVORA Dental Disc 2 (JUV), and (6) direct resin composite fillings out of Tetric EvoCeram (TET). Sound teeth (7) acted as positive control group. Half of the specimens of each group ($n = 8$) were treated in a chewing simulator combined with thermal cycling (1.2 million × 50 N; 12,000 × 5 °C/55 °C). Fracture load and fracture types of all molars were determined. Statistical analyses using Kolmogorov-Smirnov test and two-way ANOVA with partial eta squared (η_p^2) followed by Scheffé post hoc test, chi square test and Weibull modulus m with 95% confidence interval were computed ($p < 0.05$).

Results ESS and TET demonstrated the lowest fracture load with a minimum of 956 N, whereas sound molars showed the highest values of up to 2981 N. Chewing simulation indicated no impact ($p = 0.132$). With regard to Weibull modulus, KET presented a lower value after chewing simulation than JUV, whereas TET had the highest value without chewing simulation. All indirect restorations revealed a tooth fracture (75–100%), direct resin composite fillings showed a restoration fracture (87.5%), and 50% of the sound teeth fractured completely or had cusp fractures.

Conclusions All 3D printed and milled indirect PEEK inlays as well as the direct resin composite fillings presented a higher fracture load than the expected physiological and maximum chewing forces.

Clinical relevance 3D printing of inlays out of PEEK via FLM provided promising results in mechanics, but improvements in terms of precision and esthetics will be required to be practicable in vivo to represent an alternative dental material.

Keywords PEEK · 3D printing · Additive manufacturing · Fused layer manufacturing (FLM) · Chewing simulation · Fracture load

Introduction

Additive manufacturing (AM), also known as rapid prototyping, includes the manufacturing by 3D printing and enables the development of new material classes with more efficient and material-saving fabrication processes. Already today, 3D printing has a wide range of applications, such as dental restorations, implants, surgical guides, orthodontic devices, and physical models [1]. AM is also applied successfully in dental research, education, and training [2].

There are many advantages of 3D printing in dentistry, which improve the daily work of a dentist or dental technician and also the quality of patient life [3]. One of the biggest advantages is that patient-individual parts can be developed and produced with a minimum of time, amount of material, and cost. The mostly required postprocessing (e.g., removal of support structures, surface polishing) and an anisotropic behavior (mechanical properties depend on the printing direction) have to be mentioned as disadvantages [4].

✉ Alexander Prechtel
Alexander.Prechtel@med.uni-muenchen.de

[1] Department of Prosthetic Dentistry, Ludwig-Maximilians-Universität Munich, Goethestrasse 70, 80336 Munich, Germany

[2] Department of Conservative Dentistry and Periodontology, Ludwig-Maximilians-Universität Munich, Goethestrasse 70, 80336 Munich, Germany

Published online: 27 January 2020

AM is used in a digital workflow since the 1980s and consists of data acquisition (e.g., intraoral scan of patient teeth), designing the desired object by a CAD (computer-aided-design) software, dividing the object into many layers by a slicing software, and finally computer-aided manufacturing (CAM) with a 3D printing machine [5]. There are several different 3D printing techniques in dentistry such as stereolithography (SLA), selective laser sintering (SLS), digital light processing (DLP), and fused layer manufacturing (FLM) [4]. Since 2013, FLM is suitable for processing high-performance polymers from the group of polyaryletherketone (PAEK) [6]. PAEKs are semi-crystalline linear aromatic thermoplastics, whereby the number of ether and ketone bindings provides different variants, such as polyetherketoneketone (PEKK) and polyetheretherketone (PEEK), which have slightly different mechanical and thermal properties. In dentistry, PEEK is most common since it has outstanding properties, such as excellent biocompatibility, non-cytotoxical and bio-inert behavior, favorable mechanical properties, radio translucency, bone-like Young's modulus of 3–4 GPa and low plaque affinity and chemical stability [7]. Until now, PEEK has been used in dentistry for removable and fixed dental prostheses, implants, and implant abutments as well as orthodontic devices [8], whereas in literature, it is mostly mentioned in relation to prosthetics [9]. PEEK was predominantly processed out of industrially pre-pressed pellets or granular form and CAD/CAM-supported milled out of prefabricated blanks. Producing dental restorations additively via FLM out of PEEK is still hardly widespread. With the FLM technique, the solid PEEK filament is melted in a nozzle and placed layer by layer onto the building platform in a specific laydown pattern. Critical factors are the required continuously high temperatures of over 350 °C, a special heat management of the nozzle, building platform and chamber to avoid nozzle blockage or material degradation and to achieve firm layer bonding as well as low component warpage [10].

Most restorative procedures involve massive reductions of tooth structure as the teeth have to be prepared. For example, when preparing class II cavities for an indirect restoration, more tooth structure is lost compared with preparations for direct restorations, which results in a lower tooth fracture strength [11]. Thus, occlusal preparations with a width of one-third of the intercuspal distance weaken the strength of a tooth by 60% [12]. However, indirect restorations offer some advantages over direct ones, such as better proximal and occlusal designs, higher wear resistance, superior mechanical properties, and more precise marginal adaptation, resulting in reduced microleakage [13].

Weibull statistics is particularly suitable in dental material research to characterize the failure and reliability of brittle materials such as ceramics and polymers [14]. The Weibull modulus m is a parameter for the dispersion of the strength values and provides information about the structural homogeneity of one material [15].

Besides this parameter, fracture load and durability to thermal stress are important factors that should be investigated before applying a new dental material in order to achieve an optimal clinical performance and a high long-term success.

Therefore, measuring fracture load and using a chewing simulator are proven in vitro methods to simulate mechanical properties of the material under masticatory movement and force effectively [16].

The aim of this study was to investigate the impact of chewing simulation combined with thermocycling on the fracture load of different 3D printed class I inlay materials compared with one milled PEEK material, one conventional direct resin composite material, and sound teeth. The null hypotheses tested were (1) the various restoration materials show no differences in the fracture load and (2) the fatigue process of chewing simulation has no impact on the fracture load of the restored teeth.

Materials and methods

A total number of 112 human maxillary and mandibular extracted molars free of visible cracks, carious lesions, or restorative materials were collected for this study, which were stored in 0.5% chloramine T trihydrate (Carl Roth, Karlsruhe, Germany, CAS-No: 7080-50-4; Lot-No: 285228116) at room temperature (23 °C) for a maximum of 1 week after extraction and then in distilled water at 5 °C. All teeth were thoroughly cleaned, and their roots were embedded up to the cemento-enamel junction (CEJ) in a self-cured acrylic resin (ScandiQuick A and B, ScanDia, Hagen, Germany, Lot-No: 09201 and 09202) in round metal molds (Fig. 1a). Before measurement, the embedded molars were stored in distilled water at 37 °C in an incubator (HeraCell 150, Heraeus, Hanau, Germany), which was changed every week. All molars were randomly divided into seven groups ($n = 16$ teeth) with different restoration materials (Table 1). Occlusal class I cavities (vestibular-oral width of 3.0 mm, distal-mesial width of 6.5 mm, occlusal reduction of 4.0 mm, convergence angle of 6°) were prepared, except one group that served as an unprepared and unrestored control group. The preparations were made under permanent water cooling at 40,000 min^{-1}/rpm with a conical diamond bur (6848.314.031, Gebr. Brasseler, Lemgo, Germany) in a high-speed handpiece (Perfecta 900, W&H, Laufen, Germany), which was mounted in a dental parallel surveyor (F4 basic, DeguDent GmbH, Hanau, Germany). Care was taken to always prepare cavities of the same size and depth, which was ensured with markings on tooth and bur (Fig. 1a). The molars were subsequently restored with indirect and direct restorations.

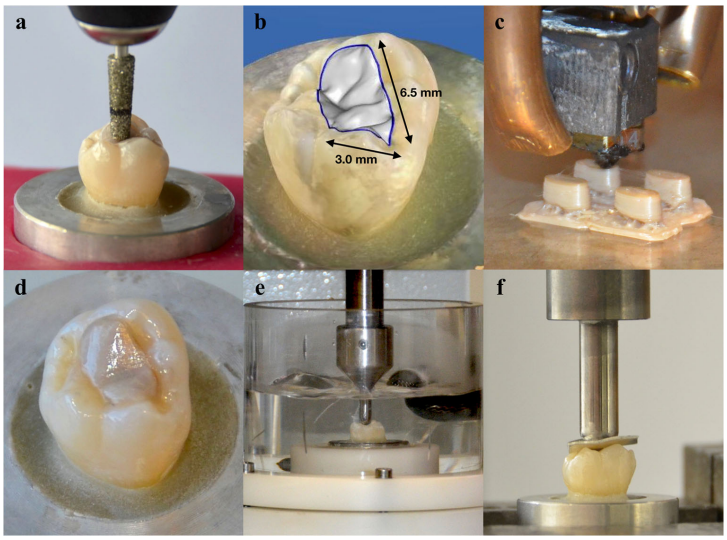

Fig. 1 Workflow. **a** Preparation of a class I cavity. **b** Designing an inlay by CAD software. **c** Printing via FLM. **d** Adhesively inserted inlay. **e** Chewing simulation. **f** Fracture load measurement

For this purpose, the prepared teeth for the indirect restorations were scanned with an optical 3D camera (CEREC Omnicam, Dentsply Sirona, Bensheim, Germany), inlays were designed by a CAD software (CEREC SW 4.6.1, Dentsply Sirona), and files were created in STL format (inLab CAD SW 18.1, Dentsply Sirona) (Fig. 1b). From each printable PEEK material (Essentium PEEK (ESS), KetaSpire PEEK MS-NT1 (KET), VESTAKEEP i4 G (VES), and VICTREX PEEK 450G (VIC)) (Table 1), 16 inlays were additively manufactured out of a filament (diameter 1.75 mm) via FLM with the printer HTRD1.2 (KUMOVIS, Munich, Germany) (Fig. 1c). Before manufacturing, the filament was dried in an oven (Heraeus RT 360, Heraeus) at 120 °C for 12 h in order to extract moisture and avoid artefacts such as air inclusions [6]. For better comparability, all materials were printed with the same parameters (Table 2). After the printing process was finished, the inlays were immediately removed from the building platform and cooled down at room temperature. Thus, support structures had to be removed with milling instruments (H73EF.104.014 and H136EF.104.016, Gebr.

Table 1 Summary of used materials, abbreviations, compositions, manufacturer, and lot numbers

	Material	Abbreviation	Composition	Manufacturer	Lot no
3D printed indirect PEEK inlays	Essentium PEEK	ESS	Polyetheretherketon, unfilled	Essentium Inc., Pflugerville, USA	1-80601
	KetaSpire® PEEK MS-NT1	KET	Polyetheretherketon, unfilled	Solvay Specialty Polymers USA, L.L.C., Alpharetta GA, USA	1850009004
	VESTAKEEP® i4 G (exp. material)	VES	Polyetheretherketon, unfilled	Evonik Industries AG, Essen, Germany	"testing grade" version
	VICTREX® PEEK 450G	VIC	Polyetheretherketon, unfilled	Victrex plc., Thornton Cleveleys, UK	7082
Milled indirect PEEK inlays	JUVORA™ Dental Disc 2	JUV	Polyetheretherketon, unfilled	JUVORA Ltd., Thornton Cleveleys, UK	WO000042IDML
Direct resin composite fillings	Tetric EvoCeram®	TET	BisGMA, UDMA, DMDMA, Bariumglass, YbF_3, mixed oxide, pre-polymerized fillers	Ivoclar Vivadent GmbH, Schaan, Liechtenstein	Y08778
Control group	Sound human molars	-	-	-	-

BisGMA, bisphenol-A-diglycidyldimethacrylate; *DMDMA*, decamethylendimethacrylate; *UDMA*, urethane dimethacrylate; *YbF_3*, ytterbiumtrifluorid

Table 2 Printing parameters and technical specifications of HTRD1.2

Nozzle temperature	390 °C
Nozzle diameter	0.4 mm
Heated building chamber	100 °C
Cooling temperature	120 °C
Heated building platform	220 °C
Ventilation	Heated laminar airflow
Layer height	0.15 mm
Extrusion width	0.30 mm
Printing speed	300 mm/min

Brasseler) in a handpiece (KaVo EWL K9, KaVo Dental, Biberach/ Riß, Germany), the inlay had to be adapted individually to its cavity, and the occlusal surface had to be re-contoured (Fig. 2). Such postprocessing also had to be performed on the milled inlays made out of JUVORA Dental Disc 2 (JUV) (Table 1). These were milled out of a disc with a CAD/CAM milling machine (ZENOTEC 4030, Wieland Dental + Technik, Pforzheim, Germany).

After all inlays had been adequately adapted, they were adhesively inserted into the cavities. All inlays were air-abraded with 50-µm Al_2O_3 powder under 0.2 MPa for 10 s at a distance of 10 mm and in an angle of 45° (basic Quattro IS; Renfert, Hilzingen, Germany), conditioned with a thin film of visio.link (bredent, Senden, Germany) and light-cured for 30 s (bre. Lux LED N, bredent). The tooth-hard tissues were pre-treated using total etch technique, in which the enamel was etched for 30 s and the dentin for 15 s with a 35% phosphoric acid (H_3PO_4) (Total Etch, Ivoclar Vivadent, Schaan, Liechtenstein). Thereafter, according to the manufacturer's instructions, Syntac Primer (Ivoclar Vivadent) was applied for at least 15 s, Syntac Adhesive (Ivoclar Vivadent) for 10 s, and both were gently air-dried. Subsequently, a thin layer of Heliobond (Ivoclar Vivadent) was applied in all cavities and light-cured for 10 s (Elipar S10, 3M, Seefeld, Germany) only for the direct composite fillings. The dual-curing Variolink Esthetic (shade warm+, Ivoclar Vivadent) was used as luting resin composite for the inlays, which was light-cured occlusally for at least 20 s (Elipar S10, 3 M) after the inlay was inserted. Finally, the bonded inlays were polished to high gloss with goat hair brushes (bredent) and polishing paste (Abraso Starglanz, bredent) for 1 min at 3000 min^{-1}/rpm (KaVo EWL K9, KaVo Dental) (Fig. 1d).

The direct restorations were performed with the nanohybrid resin composite Tetric EvoCeram (TET) (shade A3, Ivoclar Vivadent) (Table 1). The cavities were filled using an incremental filling technique, where each layer (max. 2 mm) was light-cured for 20 s (Elipar S10, 3M). The polishing was carried out with a two-step polishing system (94028M.204.130 and 94028F.204.130, Gebr. Brasseler) for 1 min at 6000 min^{-1}/rpm under permanent water cooling.

Eight teeth were selected from each of the seven groups. They were mounted in a chewing simulator (CS-4.8, SD Mechatronics, Feldkirchen-Westerham, Germany) for 1.2 million masticatory cycles with a frequency of 1.20 Hz and force of 50 N (Fig. 1e). The chambers were filled alternately for 12,000 cycles for 30 s each with 5 and 55 °C distilled water, so that in addition to mechanical loading, thermal cycling also took place simultaneously. Stainless steel balls out of chromium-nickel 1.4301 (diameter: 4.5 mm; SD Mechatronics) were used as antagonists and were aimed at a three-point occlusal contact. They moved in vertical (1.0 mm) and lateral (0.7 mm) directions as it occurs during physiological chewing. Subsequently, each single tooth was examined under a light microscope (Leica DM2700 M, Leica Microsystems GmbH, Wetzlar, Germany) for fractures that might have occurred during mechanical and thermal exposure. After this simulation, fracture load measurements were performed in a universal testing machine (Zwick 1445, ZwickRoell, Ulm, Germany). The embedded tooth was fixed into the holding device of the machine, and a tin foil (thickness 0.5 mm; DENTAURUM, Ispringen, Germany, Lot-No: 469721) was placed between the stamp and the tooth to ensure a homogenous force distribution and to avoid local force peaks (Fig. 1f). Then, an increasing load was applied perpendicularly to the central fossa with a stamp of hemispherical shape (diameter 6 mm) until failure occurred (crosshead speed 1 mm/min). Force values were recorded

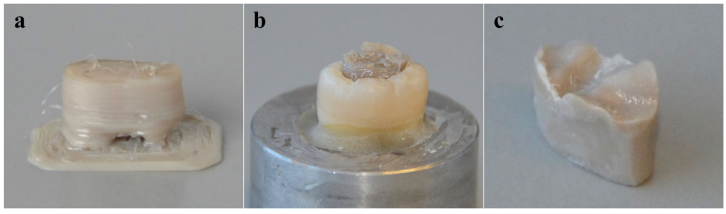

Fig. 2 Postprocessing of the printed inlays. **a** Removing of support structure. **b** Adaptation to the cavity. **c** Occlusal re-contouring

automatically in Newton (N) as soon as the maximum fracture load decreased by 50% until an initial crack or total fracture was detected (testXpert II V3.6, ZwickRoell). The fracture types were classified as follows: tooth fracture (a), cusp fracture (b), and restoration fracture (c) (Table 5).

All measured data were analyzed with the SPSS statistic program (version 25.0.0.1, IBM, Armonk, NY, USA). The assumption of normality was tested using Kolmogorov-Smirnov test. Two-way ANOVA with partial eta squared (η_p^2) followed by Scheffé post hoc test was computed to verify the impact of chewing simulation on fracture load. Weibull distribution parameter (Weibull modulus m) was calculated using the maximum likelihood estimation method and 95% confidence interval (95% CI) [17]. Chi square (chi^2) test and Ciba-Geigy tables were used to analyze the relative frequencies of fracture types together with the corresponding 95% confidence intervals (CI) [18]. In all analyses, the level of significance was set to $p < 0.05$.

Results

The descriptive statistics is shown in Table 3. The Kolmogorov-Smirnov test indicated no violation of normal distribution, so data were analyzed parametrically. According to two-way ANOVA, the restoration material showed an influence on the fracture load ($p < 0.001$), whereas chewing simulation had no impact ($p = 0.132$) (Table 4).

ESS and TET showed the significant lowest fracture load down to a minimum of 956 N (Fig. 3). VIC was together with VES, KET, and JUV in the same value range. The sound molars presented the highest fracture load values of up to 2981 N ($p < 0.001$).

The microscopic examinations showed that the chewing simulation combined with thermal cycling did not cause any fractures in all investigated teeth.

Regarding Weibull modulus, KET had a significantly lower value than JUV for the groups with performed chewing simulation, whereas TET showed for the groups without chewing simulation the significant highest Weibull modulus (Table 3).

With respect to fracture types, differences between the groups were observed (chi^2 test $p < 0.001$). All indirect restorations and sound molars, regardless of the fatigue process, showed a significantly higher tooth fracture rate (75–100%) than TET (Table 5). All 3D printed inlays remained intact after the fracture load test (100%). Only one milled inlay out of JUV failed due to a restoration fracture (12.5%). TET showed a significantly higher restoration fracture rate than all the other groups (87.5%). With regard to cusp fractures, the untreated molars presented the significantly highest relative frequencies (50%).

Discussion

This study investigated the fracture load of 3D printed indirect PEEK inlays in comparison with milled ones, conventionally direct composite fillings, and sound human molars under the influence of chewing simulation with combined thermal cycling. In general, all tested indirect and direct restorations demonstrated a higher fracture load compared with the expected physiological chewing forces of 110–125 N [19, 20] and maximum bite forces in the molar region of up to 909 N [21, 22]. However, the first null hypothesis had to be rejected, since the various materials indicated differences in fracture

Table 3 Fracture load (mean ± standard deviation) and Weibull modulus (95% confidence intervals) according to the restoration material and fatigue process

Restoration material	With chewing simulation			Without chewing simulation		
	Mean ± SD (in *N*)	95% CI (in *N*)	Weibull modulus (95% CI)	Mean ± SD (in *N*)	95% CI (in *N*)	Weibull modulus (95% CI)
Essentium PEEK	956 (± 222)^{a}	769.1; 1151	4.2 (1.9; 8.6)^{AB}	1062 (± 300.4)^{a}	809.8; 1323	4.1 (1.8; 8.5)^{AB}
KetaSpire PEEK MS-NT1	1715 (± 571.3)^{bc}	1227; 2202	2.7 (1.2; 5.6)^{A}	1681 (± 416.8)^{bc}	1323; 2039	4.4 (2.0; 9.2)^{AB}
VESTAKEEP i4 G	1712 (± 325.0) *^{bc}	1430; 1993	5.3 (2.4; 11.0)^{AB}	1633 (± 431.0)^{bc}	1262; 2003	3.8 (1.7; 7.9)^{AB}
VICTREX PEEK 450G	1392 (± 444.1)^{bc}	1010; 1773	3.4 (1.5; 7.0)^{AB}	1800 (± 324.8)^{bc}	1518; 2081	6.3 (2.9; 13.0)^{AB}
JUVORA Dental Disc 2	1984 (± 291.9)^{c}	1730; 2238	7.4 (3.4; 15.3)^{B}	1756 (± 511.2)^{c}	1318; 2193	3.4 (1.5; 7.1)^{AB}
Tetric EvoCeram	1189 (± 307.9)^{ab}	930.8; 1456	3.7 (1.6; 7.6)^{AB}	1277 (± 181.6)^{ab}	1115; 1439	7.7 (3.2; 16.0)^{B}
Sound human molars	2385 (± 583.8)^{d}	1886; 2883	3.8 (1.7; 8.0)^{AB}	2981 (± 706.9)^{d}	2379; 3581	4.3 (1.9; 8.9)^{AB}

*Indicate deviation of the normal distribution

$^{a–d}$ Indicate significant differences between fracture load among all tested groups regardless of the fatigue process

^{AB} Indicate significant differences between Weibull modulus among all tested groups within one fatigue process

Table 4 Two-way ANOVA results of fracture load according to the restoration material and chewing simulation

	Sum of squares	*df*	Mean squares	*F*	*p*	η_p^2
Restoration material	27,194,106	6	4,532,351	24.9	< 0.001	0.604
Chewing simulation	419,245	1	419,245	2.30	0.132	0.023
Restoration material × chewing simulation	1,980,256	6	330,043	1.81	0.104	0.100
Error	17,837,880	98	182,019			
Total	363,620,932	112				

load. ESS and TET showed the lowest fracture load of all tested groups. Although ESS was processed like all the other filaments as well as the inlays were inserted according to the same procedure, the low fracture load might be explained by the material composition, like lower filler degree or different filler types for example. Unfortunately, this is difficult to state due to a lack of information by the manufacturer. It might also be possible that each filament needs individual printing parameters to achieve better mechanics. Since the printed components have an anisotropic behavior, the printing direction and thus the position of the support structure can decisively influence the mechanical properties. In the present study, the support structure was attached to the occlusal surface of the inlay, whereby the printing direction was parallel to the direction of measurement of the fracture load, which is supposed to lead to optimal mechanics [23].

TET also had the lowest fracture load, because direct composite fillings placed in a cavity in several layers often exhibit a degree of inhomogeneity in form of small voids, insufficiently polymerized parts, and polymerization shrinkage stress, resulting in lower mechanics [24]. Also, because of a higher polymer content than the semi-crystalline PEEK materials, the water absorption is higher. This might explain that the resin composite reacted sensitively to the water storage and chewing simulation with thermal cycling [25].

The sound molars presented by far the highest fracture load. Unfortunately, cavity preparations usually lead to an extended loss of enamel and dentin. As a consequence, the tooth loses considerable stability and becomes more vulnerable to fractures. Mondelli et al. have found out that a class I cavity reduces the strength of the tooth less than a class II preparation with equal width, so marginal ridges provide a tooth stability [26]. The buccolingual width is also an influential factor on flexural strength. In the present investigation, the width was maximum one-third of the intercuspal distance. However, even with this narrow occlusal cavity, the tooth is already weakened compared with an uncavitated tooth [12]. The etiology of a tooth fracture is complex and multifactorial. While intact teeth therefore rarely fracture under chewing load, teeth weakened by preparation of cavities, caries, endodontic treatments, genetic disorders like amelo-/dentinogenesis imperfecta or molar-incisor hypomineralization (MIH) and periodontal lesions may spontaneously fracture under physiological mastication load, so

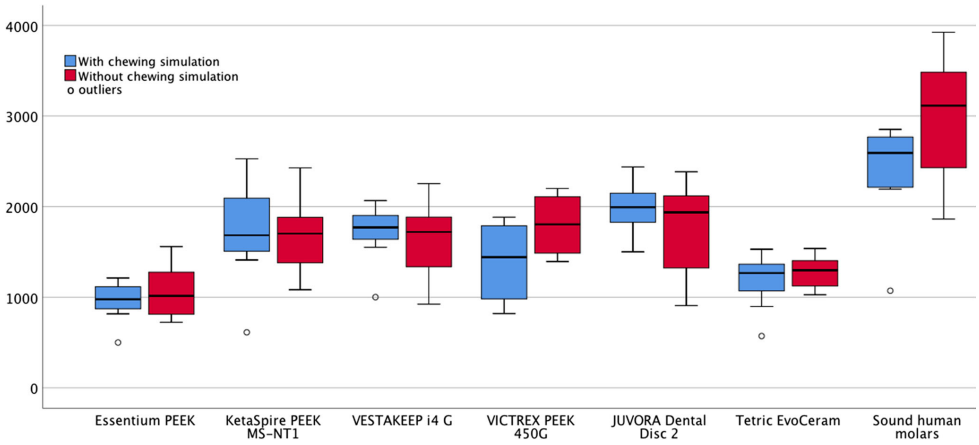

Fig. 3 Fracture load (in *N*) of all tested materials with and without chewing simulation presented in boxplot

Table 5 Relative frequencies (95% confidence intervals) of the fracture types according to the restoration material and fatigue process

				
Restoration material	Fatigue process	**Tooth fracture (%)**	**Cusp fracture (%)**	**Restoration fracture (%)**
Essentium PEEK	With chewing simulation	100 (62; 100)[c]	0 (0; 37)[a]	0 (0; 37)[a]
	Without chewing simulation	87.5 (46; 100)[c]	12.5 (0; 53)[a]	0 (0; 37)[a]
KetaSpire PEEK MS-NT1	With chewing simulation	100 (62; 100)[c]	0 (0; 37)[a]	0 (0; 37)[a]
	Without chewing simulation	100 (62; 100)[c]	0 (0; 37)[a]	0 (0; 37)[a]
VESTAKEEP i4 G	With chewing simulation	87.5 (46; 100)[c]	12.5 (0; 53)[a]	0 (0; 37)[a]
	Without chewing simulation	100 (62; 100)[c]	0 (0; 37)[a]	0 (0; 37)[a]
VICTREX PEEK 450G	With chewing simulation	100 (62; 100)[c]	0 (0; 37)[a]	0 (0; 37)[a]
	Without chewing simulation	100 (62; 100)[c]	0 (0; 37)[a]	0 (0; 37)[a]
JUVORA Dental Disc 2	With chewing simulation	100 (62; 100)[c]	0 (0; 37)[a]	0 (0; 37)[a]
	Without chewing simulation	75 (33; 97)[b]	12.5 (0; 53)[a]	12.5 (0; 53)[a]
Tetric EvoCeram	With chewing simulation	0 (0; 37)[a]	12,5 (0; 53)[a]	87,5 (46; 100)[b]
	Without chewing simulation	12.5 (0; 53)[a]	0 (0; 37)[a]	87.5 (46; 100)[b]
Sound human molars	With chewing simulation	50 (14; 85)[b]	50 (14; 85)[b]	0 (0; 37)[a]
	Without chewing simulation	87.5 (46; 100)[c]	12.5 (0; 53)[a]	0 (0; 37)[a]

[a–c] Indicate significant differences between relative frequencies among all tested groups within one fracture type

that far lower forces are sufficient for failure of the tooth to occur [27]. Consequently, a major restoration or a root canal therapy is indicated or even in the worst case, the affected tooth must be extracted. Also, occlusal overloading due to bruxism, accidental trauma, adverse cusp-fossa relationship, inadequate restoration planning, manufacturing defects, or material fatigue can cause a fracture [28].

To be able to predict and prevent material failure, Weibull statistics is a convenient tool in dentistry for comparing the flaw size distribution as well as flexural strength of different specimen sizes, stress configurations, and testing conditions [14]. The Weibull modulus *m* indicates the spread of the distribution, so the higher the value, the smaller the dispersion and better the structural reliability of the material. In this study, for the groups with performed chewing simulation, the 3D printed material KET showed the lowest Weibull modulus, whereas the milled material JUV had the highest one. This could be explained by a manufacturing process of JUV under controlled industrial conditions that provides a homogeneous structure and high reliability. It is unclear why KET presented such a low Weibull modulus and thus the lowest reliability and fatigue resistance. This might be explained by a high water absorption during water storage in the incubator or chewing simulator. Unfortunately, again, data about the water absorption capacity, for example, by the manufacturer is missing.

TET showed the highest *m* value for the groups without chewing simulation, which is remarkable, as it is a direct filling material, which, due to the incremental application, always shows minimal inhomogeneities, and therefore, a low *m* value could be expected. Apparently, it was processed homogeneously in this investigation.

In terms of fracture types, all indirect restorations as well as sound molars showed tooth fractures, indicating a strong coherent connection within the restoration material respectively hard tooth tissue. The single layers of the 3D printed inlays seemed to be solidly fused due to the high melting

temperatures. The high forces applied during the test were instantly transmitted to the tooth, resulting in a fracture. As PEEK has a lower Young's modulus than dentin (13 GPa, [29]) and enamel (72.7–87.5 GPa, [30]), tensile stress is concentrated and transmitted to the tooth under axial compressive stress, which leads to fracture [31]. Although TET also has a lower Young's modulus than the tooth structure, the fillings fractured during the measurements. One explanation might be that a fracture can spread more easily between the single polymerized parts due to unavoidable minimal inhomogeneities [32].

The teeth of this study fractured completely as well as cusp fractures occurred, which is rather explained by the irregular anatomical shapes of the used molars. Each natural tooth is individual with regard to the configuration of the occlusal surface, the size of the cusps, level of calcification, and location of the pulp chamber, which all have a decisive influence on the fracture type and fracture load, also represented by a high standard deviation in this investigation. Sheen et al. observed a higher fracture load for teeth of young men and no significant differences between mandibular and maxillary teeth [33]. In future studies, teeth of almost the same size, gender, and age range should be selected for enhanced comparability.

As the results presented, there were no major differences in fracture load values between printed and milled inlays. However, the printed inlays required an intensive postprocessing care. After removing the support structures, the final occlusal surface differed from the designed one and had to be re-contoured. The basal surface and the sides of the inlay had to be adapted in quite an intensive manner for being able to insert it into the cavity. As a result, a quite large cement gap was mostly created, which is susceptible to microleakage in vivo [34]. On the other hand, it was found that the fracture load is not affected by the thickness of the cement gap and internal fit, only by the quality of the margin [35]. Apart from the good mechanical properties, the poor esthetics of the PEEK inlays has to be criticized with regard to a brownish-gray color. In order to achieve a tooth-colored translucent appearance, veneering is necessary, whereas a digital veneering method presented the highest fracture load [36].

The fact that the fracture load values exceeded the chewing forces can also be explained by the materials used for adhesive luting in this study. Thus airborne particle abrasion increases the surface area, which enables better penetration of the adhesive and ensures a solid micro-retentive bonding [37]. Due to the fact that visio.link is MMA (methyl methacrylate)-based and contains PETIA (pentaerythritol triacrylate), it has superior properties compared with other adhesive systems for PEEK [38]. The application of Syntac with Variolink is also a proven combination for adhesive luting of indirect restorations, which have achieved excellent results [39].

Fatigue resistance of dental materials is a very important factor when selecting a suitable material for a restoration, which was examined in the present study by chewing simulation. In order to increase the clinical relevance, chewing simulation with combined thermal cycling was used as an aging process in order to carry out a simultaneous mechanical and thermal stress test of the restored teeth. The 1.2 million chewing cycles applied correspond to 5 years of clinical practice and offer sufficient clinical relevance with regard to the survival rate of dental restorations [16]. Surprisingly, this fatigue process had no impact on the fracture load of the tested molars, so all materials revealed sufficient chewing resistance and the second null hypothesis had to be accepted. However, the teeth were only loaded with 50 N during the simulation, whereby physiologically higher chewing forces should rather be used. To develop a chewing simulator with a stable function using such high weights is quite a challenge. Teeth are constantly in contact with salvia in the oral environment, which was not practiced in this study. Storage and chewing simulation with physiological saliva could have yielded even better values [40].

Compared with other indirect materials, inlays out of yttrium-stabilized zirconia ceramic showed comparable fracture resistance to intact teeth of up to 1646 N due to the high compressive strength and transformation toughening of this ceramic [41]. Inlays made out of resin composite and lithium disilicate glass ceramic revealed lower values than intact teeth, whereas composite ones had the lowest fracture strength due to a minor Young's modulus of elasticity and rigidity [31].

The present investigation demonstrated the first steps towards AM of dental restorations out of PEEK via FLM and has shown promising results regarding mechanics and chewing resistance. Therefore, a huge potential in future applications can be expected. However, technical improvements on the printer side with regard to accuracy, detailed information about the filament composition to explain and predict the mechanical behavior, and in vivo clinical studies are mandatory.

Conclusion

Within the limitations of this investigation, the following conclusions can be made:

- All 3D printed and milled indirect PEEK inlays as well as the direct resin composite fillings showed a higher fracture load than the expected physiological and maximum chewing forces in the molar region, whereas sound molars demonstrated the highest fracture load of up to 2981 N.
- Chewing simulation with combined thermal cycling had no impact on the fracture load of the tested specimens.

- A quite extensive post-processing had to be executed especially for the printed inlays.
- All 3D printed PEEK indirect inlays stayed intact after the fracture load test.

Acknowledgments The authors would like to acknowledge KUMOVIS for providing the 3D printer HTRD1.2 and the PEEK filaments. We are also grateful to Ivoclar Vivadent and Gebr. Brasseler for material support of this study.

Funding Information Open Access funding provided by Projekt DEAL.

Compliance with ethical standards

Conflict of interest The authors declare that they have no conflict of interest.

Ethical approval This article does not contain any studies with human participants or animals performed by any of the authors.

References

1. Dawood A, Marti Marti B, Sauret-Jackson V, Darwood A (2015) 3D printing in dentistry. Br Dent J:521-529. https://doi.org/10.1038/sj.bdj.2015.914
2. Reymus M, Fotiadou C, Kessler A, Heck K, Hickel R, Diegritz C (2019) 3D printed replicas for endodontic education. Int Endod J 1: 123–130. https://doi.org/10.1111/iej.12964
3. Javaid M, Haleem A (2019) Current status and applications of additive manufacturing in dentistry: a literature-based review. J Oral Biol Craniofac Res 3:179–185. https://doi.org/10.1016/j.jobcr.2019.04.004
4. Ngo TD, Kashani A, Imbalzano G, Nguyen KTQ, Hui D (2018) Additive manufacturing (3D printing): a review of materials, methods, applications and challenges. Compos B Eng:172–196. https://doi.org/10.1016/j.compositesb.2018.02.012
5. van Noort R (2012) The future of dental devices is digital. Dent Mater 1:3–12. https://doi.org/10.1016/j.dental.2011.10.014
6. Valentan B, Kadivnik Z, Brajlih T, Anderson A, Igor D (2013) Processing poly (ether etherketone) on a 3d printer for thermoplastic modelling. Mater Tehnol 6:715–721
7. Kurtz SM, Devine JN (2007) PEEK biomaterials in trauma, orthopedic, and spinal implants. Biomaterials 32:4845–4869. https://doi.org/10.1016/j.biomaterials.2007.07.013
8. Haleem A, Javaid M (2019) Polyether ether ketone (PEEK) and its manufacturing of customised 3D printed dentistry parts using additive manufacturing. Clin Epidemiol Glob Health. https://doi.org/10.1016/j.cegh.2019.03.001
9. Bathala L, Majeti V, Rachuri N, Singh N, Gedela S (2019) The role of polyether ether ketone (Peek) in dentistry-a review. J Med Life 1: 5–9. https://doi.org/10.25122/jml-2019-0003
10. Vaezi M, Yang S (2015) Extrusion-based additive manufacturing of PEEK for biomedical applications. Virtual and Physical Prototyping 3:123–135. https://doi.org/10.1080/17452759.2015.1097053
11. Mondelli J, Sene F, Ramos RP, Benetti AR (2007) Tooth structure and fracture strength of cavities. Braz Dent J 2:134–138
12. Larson TD, Douglas WH, Geistfeld RE (1981) Effect of prepared cavities on the strength of teeth. Oper Dent 1:2–5
13. Coelho-de-Souza FH, Camacho GB, Demarco FF, Powers JM (2008) Fracture resistance and gap formation of MOD restorations: influence of restorative technique, bevel preparation and water storage. Oper Dent 1:37–43. https://doi.org/10.2341/07-27
14. Quinn JB, Quinn GD (2010) A practical and systematic review of Weibull statistics for reporting strengths of dental materials. Dent Mater 2:135–147. https://doi.org/10.1016/j.dental.2009.09.006
15. Weibull W (1951) A statistical distribution function of wide applicability. J Appl Mech 3:293–297
16. Rosentritt M, Behr M, van der Zel JM, Feilzer AJ (2009) Approach for valuating the influence of laboratory simulation. Dent Mater 3: 348–352. https://doi.org/10.1016/j.dental.2008.08.009
17. Bütikofer L, Stawarczyk B, Roos M (2015) Two regression methods for estimation of a two-parameter Weibull distribution for reliability of dental materials. Dent Mater 2:e33–e50. https://doi.org/10.1016/j.dental.2014.11.014
18. Geigy WT, Statistik T (1980) vol 8. CIBA-GEIGY Limited, Basel
19. Fontijn-Tekamp FA, Slagter AP, Van Der Bilt A, Van THMA, Witter DJ, Kalk W, Jansen JA (2000) Biting and chewing in overdentures, full dentures, and natural dentitions. J Dent Res 7: 1519–1524. https://doi.org/10.1177/00220345000790071501
20. Helkimo E, Carlsson G, Helkimo M (1977) Bite force and state dentition. Acta Odontol Scand 6:297–303. https://doi.org/10.3109/00016357709064128
21. Waltimo A, Könönen M (1995) Maximal bite force and its association with signs and symptoms of craniomandibular disorders in young Finnish non-patients. Acta Odontol Scand 4:254–258. https://doi.org/10.3109/00016359509005982
22. Ahlberg JP, Kovero OA, Hurmerinta KA, Zepa I, Nissinen MJ, Könönen MH (2003) Maximal bite force and its association with signs and symptoms of TMD, occlusion, and body mass index in a cohort of young adults. Cranio 4:248–252. https://doi.org/10.1080/08869634.2003.11746258
23. Rinaldi M, Ghidini T, Cecchini F, Brandao A, Nanni F (2018) Additive layer manufacturing of poly (ether ether ketone) via FDM. Compos B Eng:162–172. https://doi.org/10.1016/j.compositesb.2018.03.029
24. Aggarwal V, Logani A, Jain V, Shah N (2008) Effect of cyclic loading on marginal adaptation and bond strength in direct vs. indirect class II MO composite restorations. Oper Dent 5:587–592. https://doi.org/10.2341/07-152
25. Liebermann A, Wimmer T, Schmidlin PR, Scherer H, Loffler P, Roos M, Stawarczyk B (2016) Physicomechanical characterization of polyetheretherketone and current esthetic dental CAD/CAM polymers after aging in different storage media. J Prosthet Dent 3: 321-328.e2. https://doi.org/10.1016/j.prosdent.2015.09.004
26. Mondelli J, Steagall L, Ishikiriama A, de Lima Navarro MF, Soares FB (1980) Fracture strength of human teeth with cavity preparations. J Prosthet Dent 4:419–422. https://doi.org/10.1016/0022-3913(80)90213-9
27. Reeh ES, Messer HH, Douglas WH (1989) Reduction in tooth stiffness as a result of endodontic and restorative procedures. J

Endod 11:512–516. https://doi.org/10.1016/S0099-2399(89)80191-8
28. Lubisich EB, Hilton TJ, Ferracane J (2010) Cracked teeth: a review of the literature. J Esthet Restor Dent 3:158–167. https://doi.org/10.1111/j.1708-8240.2010.00330.x
29. Watts DC (1994) Elastic moduli and visco-elastic relaxation. J Dent 3:154–158
30. Habelitz S, Marshall SJ, Marshall GW, Balooch M (2001) Mechanical properties of human dental enamel on the nanometre scale. Arch Oral Biol 2:173–183. https://doi.org/10.1016/S0003-9969(00)00089-3
31. Costa AKF, Xavier TA, Noritomi PY, Saavedra G, Borges ALS (2014) The influence of elastic modulus of inlay materials on stress distribution and fracture of premolars. Oper Dent 4:E160–E170. https://doi.org/10.2341/13-092-l
32. Melo RA, Bispo AdSL, Barbosa GAS, Galvão MR, de Assunção IV, Souza ROdA, Borges BCD (2019) Morphochemical characterization, microhardness, water sorption, and solubility of regular viscosity bulk fill and traditional composite resins. Microsc Res Tech 9:1500–1506. https://doi.org/10.1002/jemt.23315
33. Sheen C-Y, Dong J-K, Brantley WA, Han DS (2019) A study of fracture loads and fracture characteristics of teeth. J Adv Prosthodont 3:187–192. https://doi.org/10.4047/jap.2019.11.3.187
34. Shetty M, Rajalakshmi S, Krishna Prasad D (2014) Comparison of marginal gap and microleakage in copy-milled and cad-milled zirconia copings bonded using light cure and chemical cure resin bonding systems. J Indian Prosthodont Soc 1:37–45. https://doi.org/10.1007/s13191-014-0359-x
35. Okutan M, Heydecke G, Butz F, Strub JR (2006) Fracture load and marginal fit of shrinkage-free ZrSiO4 all-ceramic crowns after chewing simulation. J Oral Rehabil 11:827–832. https://doi.org/10.1111/j.1365-2842.2006.01637.x
36. Taufall S, Eichberger M, Schmidlin PR, Stawarczyk B (2016) Fracture load and failure types of different veneered polyetheretherketone fixed dental prostheses. Clin Oral Investig 9:2493–2500. https://doi.org/10.1007/s00784-016-1777-4
37. Uhrenbacher J, Schmidlin PR, Keul C, Eichberger M, Roos M, Gernet W, Stawarczyk B (2014) The effect of surface modification on the retention strength of polyetheretherketone crowns adhesively bonded to dentin abutments. J Prosthet Dent 6:1489–1497. https://doi.org/10.1016/j.prosdent.2014.05.010
38. Stawarczyk B, Taufall S, Roos M, Schmidlin PR, Lümkemann N (2018) Bonding of composite resins to PEEK: the influence of adhesive systems and air-abrasion parameters. Clin Oral Investig 2:763–771. https://doi.org/10.1007/s00784-017-2151-x
39. Frankenberger R, Krämer N, Appelt A, Lohbauer U, Naumann M, Roggendorf MJ (2011) Chairside vs. labside ceramic inlays: effect of temporary restoration and adhesive luting on enamel cracks and marginal integrity. Dent Mater 9:892–898. https://doi.org/10.1016/j.dental.2011.05.007
40. Liebermann A, Ilie N, Roos M, Stawarczyk B (2017) Effect of storage medium and aging duration on mechanical properties of self-adhesive resin-based cements. J Appl Biomater Funct Mater 3:e206–e214. https://doi.org/10.5301/jabfm.5000362
41. Wafaie RA, Ibrahim Ali A, Mahmoud SH (2018) Fracture resistance of prepared premolars restored with bonded new lab composite and all-ceramic inlay/onlay restorations: laboratory study. J Esthet Restor Dent 3:229–239. https://doi.org/10.1111/jerd.12364

4. Diskussion

In diesem Abschnitt werden die eingangs erwähnten Untersuchungen konkret diskutiert.

4.1 Vergleich der Martensparameter von 3D-gedruckten und gefrästen PAEK Materialien in Bezug auf Druckrichtung und künstlicher Alterung

Anhand dieser Untersuchung konnte festgestellt werden, dass es Unterschiede in den Martensparametern zwischen 3D-gedruckten und gefrästen PAEK Materialien gab. Insbesondere zeigten die Druckrichtung sowie die künstliche Alterung einen erheblichen Einfluss auf die mechanischen Eigenschaften. Die Methode der Martenshärte Messung ist hervorragend dafür geeignet, um die elastische und plastische Verformung von polymerbasierten Materialien wie PAEK zu ermitteln. Außerdem können mit diesem Verfahren die Auswirkungen morphologischer Oberflächenveränderungen auf die mechanischen Eigenschaften durch Alterungsprozesse effizient bestimmt werden [36].

Es besteht ein enger Zusammenhang zwischen HM und H_{IT}, da sie sich nur in der Definition der Oberfläche und der Eindringtiefe unterscheiden [37]. H_{IT} betrachtet das plastische Materialverhalten, während E_{IT} für die elastische Leistung vergleichbar zum E-Modul steht [33].
In der durchgeführten Untersuchung wurden zunächst in Form von Vorversuchen Prüfkörper mit unterschiedlicher Druckgeschwindigkeit, Schichthöhe und Extrusionsbreite hergestellt, um adäquate Druckparameter für die Prüfkörper der eigentlichen Untersuchung ausfindig zu machen.
Dabei hatte sich bezüglich der Druckgeschwindigkeit herausgestellt, dass Geschwindigkeiten von 900 mm/min und 1.200 mm/min bezüglich HM und E_{IT} vergleichbare Werte zeigten, sodass aufgrund einer subjektiv höheren Präzision die Druckgeschwindigkeit auf 900 mm/min eingestellt wurde. Die Einstellung der Schichthöhe betrug 0,2 mm, da hierbei ein guter Kompromiss zwischen Präzision und Druckdauer gefunden wurde, nachdem die verschiedenen Schichthöhen keinen Einfluss auf die Martensparameter hatten. Die Extrusionsbreite wurde auf 0,4 mm justiert, da dies der

Größe der Druckdüse genau entsprach. Dadurch mussten die gedruckten Bahnen nicht künstlich verbreitert oder verschmälert werden.

Es soll besonders hervorgehoben werden, dass die gefrästen Prüfkörper höhere Martensparameter aufwiesen als die gedruckten Varianten. Dieses Ergebnis kann durch die standardisierten industriellen Herstellungsbedingungen unter einem kontrollierten Kristallisationsprozess des thermoplastischen Materials erklärt werden. Bei den gedruckten Prüfkörpern wurde das PEEK-Filament im Druckkopf geschmolzen und unterlag nach dem Druckvorgang einer mehr oder weniger kontrollierten Kristallisation, die von vielen Faktoren beeinflusst werden kann.

Ein bedeutender Faktor ist der Umgang mit den Temperaturen und das Verfahren der Abkühlung. In der durchgeführten Untersuchung wurden die gedruckten Prüfkörper unmittelbar nach dem Druckvorgang von der Bauplattform des Druckers entnommen und anschließend langsam bei Raumtemperatur abgekühlt. Hierbei stellt sich die Frage, welche Auswirkungen auf die mechanischen Eigenschaften zu erwarten gewesen wären, wenn das Bauteil nach dem Druckvorgang noch eine Zeit lang im beheizten Bauraum belassen oder unvermittelt abgekühlt werden würde. Da PAEK Werkstoffe einen geringen Kristallisationsgrad aufweisen, sind ihre mechanischen Eigenschaften von der Kristallinität abhängig [38]. Es wäre zu erwarten, dass Bauteile mit einer Wärmenachbehandlung ein besseres mechanisches Verhalten aufweisen, da das Material nach dem Druckprozess noch weiter kristallisieren und somit eine Kaltkristallisation verhindert werden kann [32]. Andererseits würde eine zu schnelle Abkühlung einen geringeren Kristallisationsgrad hervorrufen und es könnten aufgrund der starken Temperaturveränderung Risse im Bauteil entstehen [39]. Valentan et al. [7] beobachteten allerdings eine abnehmende Zugfestigkeit, wenn das Bauteil nach dem Druckvorgang für weitere 12 Stunden im noch beheizten Bauraum belassen wird. Folglich sollte dieses unverzüglich nach Beendigung des Druckprozesses aus dem Drucker entnommen werden, um die besten mechanischen Eigenschaften zu erreichen und zu erhalten.

Eine weitere Ursache für die geringen Martensparameter der gedruckten Prüfkörper könnten die vielen Artefakte wie Lufteinschlüsse und Hohlräume sein, die das Bauteil mechanisch schwächen.

Diese sind ein Hinweis auf einen erhöhten Wassergehalt im Filament, da das Material während des langen Druckvorgangs Feuchtigkeit aus der Umgebungsluft aufgenommen hat [7]. Daher wäre ein Drucker mit einer vor Feuchtigkeit geschützten Kammer für die Filamentspule erforderlich, um den vorgetrockneten Zustand aus dem Trocknungsofen während des Druckvorgangs gewährleisten zu können.

Beim Vergleich der verschiedenen Materialien zeigte ESS unabhängig von der künstlichen Alterung und der Druckrichtung die höchsten Martensparameter, während VIC die geringsten Werte hervorbrachte. Eine passende Erklärung hierfür zu finden, gestaltet sich kompliziert, da die Hersteller kaum technische Informationen über ihre Werkstoffe bereitstellen, bis auf die Tatsache, dass beide Materialien keine Füllstoffe enthalten. VIC wurde grundsätzlich für den traditionellen Spritzguss entwickelt und optimiert. Aus experimenteller Erfahrung, die während oben genannter Vorversuche gewonnen wurde, konnte ein schwächerer Verbund zwischen den übereinandergelegten Schichten festgestellt werden. Daraus lassen sich die geringen Martensparameter der vertikal gedruckten Prüfkörper aus VIC schlussfolgern.

Grundsätzlich erzielten unabhängig vom verwendeten Material und der künstlichen Alterung in horizontaler Richtung gedruckte Prüfkörper höhere Martensparameter als die in vertikaler Richtung. Dies ist dadurch zu erklären, dass bei letzteren die Richtung der Eindringpyramide während der Messung parallel zu den gedruckten Schichten erfolgte und somit zufällig exakt im Spalt zwischen zwei Schichten gemessen wurde. Folglich wurden geringe Zugspannungen erzeugt, die zu einer minimalen Abspaltung der Schichten führten [40].
Bei den horizontal gedruckten Prüfkörpern intrudierte die Pyramide senkrecht zu den Schichten. Dadurch wurde aufgrund der kleinen Größe der Pyramide und der geringen Eindringtiefe nur innerhalb einer Schicht gemessen und Zugspannungen traten nicht auf. Außerdem ist der kohäsive Verbund innerhalb der gleichen Schicht höher als der adhäsive zwischen übereinandergelegten Schichten [41]. Diese Erkenntnis wird durch die Untersuchungen von Rinaldi et al. [32] in Zugversuchen ebenfalls bestätigt, dass in horizontaler Richtung gedruckte Prüfkörper bessere mechanische Eigenschaften aufwiesen als in vertikaler Richtung.

Die Lasteindringkurven der gedruckten Prüfkörper imponierten mit stark voneinander abweichenden Kurvenverläufen, was ein Zeichen für unterschiedliche Eindringarbeiten und Martensparameter zwischen den einzelnen Prüfkörpern innerhalb desselben Materials darstellt.
Obwohl für jeden Druckprozess exakt die gleichen Druckparameter eingestellt wurden, könnten trotzdem jeweils minimal andere Umgebungsbedingungen vorgelegen haben, wie beispielsweise durch eine abweichende Raumtemperatur und Luftfeuchtigkeit, eine manuell eingestellte Z-Höhe des Druckkopfes wie auch ein manchmal erforderlicher Austausch der Druckdüse oder Glasplatte der Bauplattform. Um die unterschiedlichen PEEK-Filamente allerdings adäquat miteinander vergleichen zu können, wurde jedes Material mit den gleichen Druckparamatern verarbeitet. Möglicherweise wäre es angebracht für jedes Material ausführlich individuelle Paramater zu ermitteln, um die bestmöglichen Druckbedingungen und höchsten mechanischen Eigenschaften zu generieren.

Unter den gefrästen Prüfkörpern zeigte BHD, das mit 30 % Titandioxid (TiO_2) gefüllt ist, unabhängig von der künstlichen Alterung die höchsten Martensparameter. Durch den Zusatz von Füllstoffen, wie TiO_2, Aluminiumoxid (Al_2O_3), Siliziumdioxid (SiO_2) oder Carbonfasern, können PAEK Werkstoffe verstärkt werden. Dies führt zu höheren mechanischen Eigenschaften, aber zu schlechteren ästhetischen Ergebnissen. Nicht jede beliebige Zusammensetzung kann daher für ästhetische Restaurationen eingesetzt werden [42, 43]. Aufgrund eines verringerten Füllstoffgehalts bei DEN und BHW mit nur 20 % TiO_2 zeigten sich geringere Martensparameter, währenddessen ULT die geringsten Werte aufwies. Dies kann dadurch erklärt werden, dass ULT keine Füllstoffe enthält. Allerdings lagen keine weiteren Informationen über die genaue chemische Zusammensetzung und technische Eigenschaften offiziell vor.

Beim Vergleich mit anderen CAD/CAM-Restaurationsmaterialien, zeigten Keramiken mit Abstand die höchsten Martensparameter und PMMA-basierte Kunststoffe die geringsten Werte [35]. Die PAEK Werkstoffe der vorliegenden Untersuchung wiesen geringfügig höhere Werte auf, als die PMMA-basierten Kunststoffe.

In der Zahnmedizin ist es sehr wichtig, Restaurationsmaterialien mit einer hohen klinischen Leistungsfähigkeit einzusetzen, da diese bei der Flüssigkeits- und Nahrungsaufnahme sowie beim Atmen ständig einer feuchten Umgebung mit dynamischen Temperaturschwankungen ausgesetzt sind. Um diese klinische Situation unter Laborbedingungen entsprechend simulieren zu können, wurden für eine künstliche Alterung das Temperaturwechselbad und die Dampfsterilisation verwendet. Obwohl das Temperaturwechselbad häufig in In-vitro-Studien verwendet wird, existiert bislang kein einheitliches Versuchsprotokoll in Bezug auf Zyklenzahl, Verweildauer in den Wasserbecken und Temperaturen [44]. Bei der vorliegenden Untersuchung wurden 10.000 Zyklen eingestellt. Dies soll in etwa einem Jahr klinischen Einsatz entsprechen. Weiterhin wurden Temperaturen von 5 °C und 55 °C verwendet, da diese der physiologischen Situation am ehesten entsprechen. Die Dampfsterilisation wurde fünf Stunden lang bei 134 °C und 2 bar Druck durchgeführt. Dies soll 15 bis 20 Jahren klinischem Einsatz gleichkommen und damit über eine hohe Aussagekraft verfügen [45].

Im Allgemeinen führen thermische Belastungen in festen Werkstoffen durch Temperaturschwankungen zu Expansionen und Kontraktionen [44]. Allerdings konnten bei den untersuchten Prüfkörpern unter dem Lichtmikroskop keine entstandenen Fehlstellen wie Löcher und Risse oder Formveränderungen beobachtet werden. Ferner sind Begutachtungen unter einem Rasterelektronenmikroskop erforderlich, um die morphologischen Veränderungen durch eine künstliche Alterung präziser darstellen und dadurch die geringeren Martensparameter nach der Alterung möglicherweise erklären zu können.

Die Alterungsprozesse in der vorliegenden Studie haben ergeben, dass horizontal gedrucktes ESS und VES, vertikal gedrucktes ESS und KET, sowie gefrästes BHD, BHW, JUV und ULT besonders anfällig gegenüber der künstlichen Alterung waren. Die thermische Belastung könnte zu Mikrorissen geführt haben, wodurch Wasser während der Dampfsterilisation in die Risse eindringen konnte, sodass dadurch die Martensparameter abnahmen [46]. Bemerkenswerterweise waren die gedruckten Prüfkörper widerstandsfähiger gegenüber den hydrothermalen Einflüssen als die gefrästen Prüfkörper. Diese Beobachtung kann durch eine geringere Wasseraufnahmekapazität der PEEK-Filamente gegenüber den PAEK Ronden erklärt werden. Leider liegen auch hierüber vonseiten der

Hersteller keinerlei Informationen vor. Im Vergleich zu anderen Materialien wie Verbundwerkstoffe, Komposite und PMMA-basierte Materialien, weist PEEK jedoch die geringste Wasseraufnahmekapazität auf [47].

Zukünftige Forschung erfordert thermodynamische und rasterelektronenmikroskopische Untersuchungen der PEEK-Filamente, um das unterschiedliche mechanische Verhalten fundiert erklären zu können. Darüber hinaus müssen die verwendete FLM-Druckereinheit und die meisten PEEK-Filamente noch in Bezug auf das Medizinproduktegesetz eingestuft werden, damit in vivo Studien durchgeführt und ein klinischer Einsatz von 3D-gedruckten PEEK Restaurationen ermöglicht werden können.

4.2 Bruchlast von 3D-gedruckten PEEK Inlays im Vergleich zu gefrästen PEEK Inlays, direkten Komposit-Füllungen und nicht restaurierten Zähnen

Diese Untersuchung verglich die Bruchlast von 3D-gedruckten indirekten PEEK Inlays im Vergleich zu gefrästen indirekten PEEK Inlays, konventionellen direkten Komposit-Füllungen und gesunden, nicht restaurierten Zähnen unter dem Einfluss einer Kausimulation mit kombiniertem Thermolastwechsel.

Im Allgemeinen wiesen alle indirekten und direkten Restaurationen eine höhere Bruchlast als die zu erwartenden physiologischen Kaukräfte von 110-125 N [59, 60] und maximalen Kaukräfte von bis zu 909 N [61, 62] in der Seitenzahnregion auf. Allerdings zeigten die verschiedenen Materialien Unterschiede in der Bruchlast, wobei ESS zusammen mit TET die geringsten Bruchlasten aufwiesen. Obwohl ESS mit den gleichen Druckparametern wie die anderen PEEK-Filamente verarbeitet wurde und die Inlays nach dem gleichen Verfahren eingesetzt worden sind, könnte die niedrige Bruchlast mit der Materialzusammensetzung wie ein niedrigerer Füllgehalt oder andere Füllkörperarten zusammenhängen. Dies kann jedoch aufgrund fehlender Herstellerinformationen nicht genau evaluiert werden. Außerdem müssten für jedes Filament individuelle Druckparameter umfassend ermittelt werden, um die besten mechanischen Eigenschaften zu erzielen.
Aufgrund des anisotropen Verhaltens der gedruckten Bauteile, könnte die Druckrichtung und damit die Positionierung der Stützstrukturen ebenfalls eine entscheidende Rolle gespielt haben. In der vorliegenden Untersuchung wurde die Stützstruktur an der okklusalen Fläche des Inlays angebracht, wodurch die Druckrichtung parallel zur späteren Messrichtung der Bruchlast war. Dies führte zu einer hohen mechanischen Leistung [32].

TET zeigte ebenfalls die geringste Bruchlast, da direkte Komposit-Füllungen in mehreren Schichten in die Kavität eingebracht werden, wodurch oft kaum vermeidbare Inhomogenitäten in Form von kleinen Lufteinschlüssen, unzureichend polymerisierten Anteilen und der Effekt der Polymerisationsschrumpfung auftreten. Dies führte zu schlechteren mechanischen Eigenschaften [63].

Des Weiteren verfügen Komposite über einen höheren Polymergehalt als die semikristallinen PEEK Werkstoffe, sodass diese anfällig gegenüber einer Wasserlagerung und der Kausimulation mit Thermolastwechsel waren [47].

Die gesunden, nicht restaurierten Molaren präsentierten mit Abstand die höchste Bruchlast, weil jegliche Zahnpräparation zu einem massiven Verlust von Schmelz und Dentin führt, wodurch der Zahn an Stabilität verliert und somit anfälliger für Frakturen wird. Mondelli et al. [64] fanden heraus, dass eine Klasse-I-Kavität bei gleicher Breite die Festigkeit eines Zahns weitaus weniger gefährdet als eine Klasse-II-Kavität, da die Randleisten einem Zahn Stabilität verleihen. Ein weiterer einfluss-reicher Faktor ist die bucco-linguale Dimensionierung der Kavitation, die in der vorliegenden Studie ein Drittel der Interkuspaldistanz betrug. Dies ist allerdings ausreichend, um den Zahn nachhaltig zu schwächen [55].

Die Ätiologie einer Zahnfraktur ist komplex und kann multifaktorielle Ursachen haben. Nachdem gesunde Zähne nur selten unter physiologischer Kaubelastung frakturieren, können geschwächte Zähne, beispielsweise durch die Präparation von Kavitäten, Karies, endodontischen Behandlungen, Mineralisationsstörungen wie Amelo-/ Dentinogenesis imperfecta oder Molaren-Inzisiven-Hypo-mineralisation (MIH) sowie parodontale Läsionen, bereits bei einer geringeren Belastung zu Bruch gehen [65]. Folglich kann anschließend eine umfangreiche Restauration, eine Wurzelkanal-behandlung oder sogar die Extraktion des betroffenen Zahnes bevorstehen. Des Weiteren können okklusale Überbelastungen durch Bruxismus, Zahntraumata, ungünstige Höcker-Fossa-Verzahnungen, fehlerhafte Restaurationsplanungen, sowie Produktionsfehler und Materialversagen zu Frakturen führen [66].
Zur Vermeidung von Letzterem kann in der dentalen Werkstoffkundeforschung durch die Weibull Statistik die strukturelle Zuverlässigkeit und die Fehlergrößenverteilung eines Werkstoffs zu-verlässig beschrieben werden. Der Weibull-Modul gibt die Breite der Verteilung an, sodass ein größerer Wert für eine geringe Streuung und somit für eine höhere strukturelle Zuverlässigkeit des Werkstoffs steht [12].

In der durchgeführten Untersuchung zeigte innerhalb der Gruppen mit ausgeführter Kausimulation gedrucktes KET den geringsten Weibull-Modul, während gefrästes JUV die höchsten Werte lieferte. Dies kann am Herstellungsprozess von JUV liegen, da dieses unter standardisierten industriellen Bedingungen gefertigt wurde, wodurch eine homogene Struktur und somit eine hohe Zuverlässigkeit gewährleistet werden kann.

Der geringe Weibull-Modul sowie die geringe Kaubeständigkeit von KET könnten an einer hohen Wasseraufnahme während der Wasserlagerung im Inkubator oder Kausimulator gelegen haben. Leider liegen auch hierbei vonseiten der Hersteller keinerlei Informationen, beispielsweise über die Wasseraufnahmekapazität der PEEK-Filamente vor, die eine schlüssige Erklärung liefern könnten.

TET präsentierte innerhalb der Gruppen ohne Kausimulation die höchsten Weibull-Module, was bemerkenswert ist, da direkte Komposit-Füllungen häufig minimale Inhomogenitäten aufweisen und somit geringere Werte zu erwarten wären. Eine Erklärungsmöglichkeit besteht darin, dass es in der durchgeführten Untersuchung äußerst homogen in die Kavität eingebracht und adäquat polymerisiert wurde.

In Bezug auf die Bruchbilder zeigten sowohl alle indirekten Restaurationen als auch die gesunden Molaren komplette Zahnfrakturen, was auf einen starken kohäsiven Verbund innerhalb des Materials respektive Zahnhartsubstanz hindeutete. Die übereinandergelegten Schichten der 3D-gedruckten Inlays wurden mithilfe der hohen Schmelztemperatur fest miteinander verbunden. Da PEEK mit 3-4 GPa [10] über ein geringeres E-Modul als Dentin (13 GPa, [67]) und Schmelz (72,7-87,5 GPa, [68]) verfügt, werden hohe axiale Druckbelastungen konzentriert und direkt auf die Zahnstruktur weitergeleitet, was zu einer Fraktur führen kann [69]. Obwohl TET ebenfalls ein geringeres E-Modul als die Zahnhartsubstanz besitzt, sind die Füllungen während der Messungen frakturiert. Dies könnte daran gelegen haben, dass sich aufgrund von oben genannten minimalen Inhomogenitäten ein Riss zwischen den einzeln polymerisierten Schichten leichter ausbreiten kann als bei monolithischen Restaurationen [70].

Die nicht restaurierten Zähne zeigten komplette Zahn- und Höckerfrakturen, was durch die unregelmäßige anatomische Morphologie erklärt werden kann. Jeder natürliche Zahn ist individuell in Bezug auf seine Kaufläche, die Größe der Höcker, den Grad an Kalzifikation sowie der Lokation

der Pulpakammer. Diese Faktoren können einen entscheidenden Einfluss auf die Bruchbilder und die Bruchlast ausüben. Sheen et al. [71] beobachteten eine höhere Bruchlast an Zähnen, die von jungen Männern stammten, und keine bedeutenden Unterschiede zwischen Ober- und Unterkieferzähnen. In zukünftigen Studien sollten daher Zähne mit ähnlicher Größe vom gleichen Geschlecht und Altersbereich für eine bessere Vergleichbarkeit verwendet werden.

Wie die Ergebnisse zeigten, waren in Bezug auf die Bruchlast zwischen den gedruckten und den gefrästen Inlays keine wesentlichen Unterschiede festzustellen. Allerdings war bei den gedruckten Inlays ein äußerst umfangreiches Postprocessing erforderlich, bei dem zunächst die Stützstruktur entfernt werden musste. Anschließend musste das Inlay seitlich und basal an die jeweilige Kavität angepasst und die Kaufläche nachkonturiert werden, da das gedruckte Inlay von dem digital gestalteten teilweise deutlich abwich. Als Folge entstand dadurch häufig ein relativ großer marginaler Randspalt, der dadurch in vivo äußerst anfällig gegenüber Mikroleakage gewesen wäre [72]. Allerdings ist bekannt, dass die Bruchlast nicht durch die interne Passung der Restauration sowie Breite des Randspalts beeinträchtigt wird, sondern von der Qualität des Randschlusses [73]. Abgesehen von den hohen mechanischen Eigenschaften der untersuchten Inlays, muss die schlechte Ästhetik von PEEK aufgrund dem bräunlich-grauen opakem Farbton bemängelt werden, weshalb für ein zahnfarbenes transluzentes Erscheinungsbild einer Restauration aus PEEK im sichtbaren Bereich eine Verblendung erforderlich ist. Dabei ergab eine digitale Verblendungstechnik die höchste Bruchlast [74].

Die Tatsache, dass die Bruchlastwerte der durchgeführten Studie oberhalb der maximal auftretenden Kaukräfte lagen, kann durchaus durch die Vorbehandlung und Konditionierung der PEEK Inlays respektive Zahnhartsubstanz sowie durch die Befestigungsmaterialien erklärt werden. Als Vorbehandlung vergrößerte ein Abstrahlen der Inlays mit Korund-Strahlgut die Oberfläche. Dies ermöglichte eine bessere Oberflächenbenetzung durch die Adhäsive, wodurch ein fester mikroretentiver Verbund geschaffen werden konnte [75]. Das verwendete Adhäsiv visio.link zeigte in mehreren Studien im Vergleich zu anderen Adhäsiven überlegene Hafteigenschaften zu PEEK, da es aufgrund von seinen MMA-(Methylmethacrylat) und PETIA-(Pentaerythrittriacrylat) Bestand-

teilen die Fähigkeit besitzt, PEEK Oberflächen zu modifizieren und für einen festen Verbund zu sorgen [75, 76]. Die Applikation des traditionellen Adhäsivsystems Syntac mit dem Befestigungskomposit Variolink ist ebenfalls eine etablierte Kombination zur adhäsiven Befestigung von indirekten Restaurationen, um ausgesprochen hohe Verbundfestigkeiten zu erzielen [77].

Bei der Wahl eines geeigneten Restaurationsmaterials spielt die Verschleißbeständigkeit eine entscheidende Rolle, welche in vorliegender Untersuchung mittels Kausimulation in Kombination mit einem Thermolastwechsel überprüft wurde, sodass ein künstlicher Alterungsprozess mit gleichzeitiger mechanischer und thermischer Belastung stattgefunden hat. Die angewandten 1,2 Millionen Kauzyklen sollen fünf Jahren klinischem Einsatz entsprechen und liefern damit eine prägnante Aussagekraft über die Überlebensrate von Restaurationen [13]. Erstaunlicherweise hat dieser Prozess keine Auswirkungen auf die Bruchlasten der untersuchten Zähne gezeigt, sodass allen verwendeten Materialien eine klinisch ausreichende Kaubeständigkeit zugesprochen werden kann. Allerdings wurden die Zähne während der Simulation nur mit einem antagonistischen Gewicht von 50 N belastet, wohingegen physiologisch weitaus höhere Kaukräfte auftreten [59]. Einen Kausimulator mit höheren Gewichten zu entwickeln und stabil zum Laufen zu bringen stellt jedoch eine ziemlich große Herausforderung dar.
In der Mundhöhle sind die Zähne ständigen Kontakt mit Speichel ausgesetzt. Diese Speichelaussetzung wurde in der durchgeführten Untersuchung nicht praktiziert. Eine Lagerung und Kausimulation mit physiologisch gewonnenem Speichel kann noch bessere Ergebnisse hervorbringen [78].

Im Vergleich zu alternativen indirekten Restaurationsmaterialien, zeigten Inlays aus yttriumstabilisiertem Zirkoniumdioxid aufgrund der hohen Druckbelastbarkeit und Phasentransformationsverstärkung dieser Keramik eine vergleichbare Frakturresistenz zu nicht restaurierten Zähnen von bis zu 1.646 N [79]. Inlays aus Harzmaterialien und Lithiumdisilikatkeramik lieferten geringere Werte als nicht präparierte Zähne, wobei Harzmaterialien aufgrund des geringen E-Moduls die geringste Bruchlast aufwiesen [69].

Abschließend kann gesagt werden, dass die durchgeführte Untersuchung die ersten Schritte auf dem Weg einer additiven Fertigung mittels FLM Technologie von dentalen Restaurationen aus PEEK aufgezeigt hat und somit ein großes Potential für zukünftige Anwendungen besitzt. Es konnten vielversprechende Ergebnisse in Bezug auf die Mechanik und die Kaubeständigkeit erzielt werden.

Allerdings sind für die Zukunft technische Verbesserungen aufseiten des Druckers bezüglich der Druckgenauigkeit, detaillierte Informationen über die PEEK-Filamente zur Erklärung und Voraussage der Mechanik als auch klinische in vivo Studien erforderlich.

5. Zusammenfassung und Ausblick

Anhand der hier zusammengefassten Untersuchungen kann festgestellt werden, dass der 3D-Druck mittels FLM Technologie von dem Hochleistungskunststoff PEEK in der Zahnmedizin das Potenzial besitzt, traditionelle Herstellungsverfahren infrage zu stellen. Vor allem der bereits etablierten subtraktiven Fertigungstechnik wird er in den kommenden Jahren eine ernst zu nehmende Konkurrenz bieten.

Obwohl gedruckte standardisierte Prüfkörpergeometrien schlechtere Martensparameter aufwiesen als gefräste Prüfkörper, zeigten sich bei den Bruchlastwerten von gedruckten und gefrästen Klasse-I-Inlays keine Unterschiede, die außerdem oberhalb der vorkommenden physiologischen und maximalen Kaukräfte lagen. Ferner kann festgestellt werden, dass die Druckrichtung und somit die Orientierung der aufeinander abgelegten Schichten einen relevanten Einfluss auf das mechanische Verhalten ausüben, indem eine senkrechte Positionierung der gedruckten Schichten zu der Belastungsrichtung die beste Mechanik hervorruft.

Während hydrothermale Alterungsprozesse einen negativen Einfluss auf die Mechanik vor allem der gefrästen Prüfkörper ausübten, zeigte die Kausimulation keinen Effekt auf die Bruchlast der restaurierten Zähne mit indirekten PEEK Inlays, was vielversprechend für eine hohe klinische Leistung und Langzeitbeständigkeit sein kann. Ein entscheidender Nachteil der gedruckten Bauteile ist die erforderliche Nachbearbeitung und die noch bestehende Unwissenheit über die genaue Zusammensetzung und das thermodynamische Verhalten der PEEK-Filamente. Auch eine Verbesserung von Druckgenauigkeit sowie Ästhetik der gedruckten Komponenten sind notwendig, um den hohen Qualitätsanforderungen in der Zahnmedizin gerecht zu werden.

Obgleich die durchgeführten Untersuchungen aussichtsreiche Ergebnisse lieferten, ist die Verarbeitung von PEEK mittels additiver Technologie in der Zahnmedizin aufgrund der hohen Anforderungen an Mechanik, Präzision sowie Ästhetik immer noch eine Herausforderung, um auch in vivo erfolgreich als ein alternatives biokompatibles Material mit diesem Herstellungsverfahren

verwendet werden zu können. Vor diesem Hintergrund sind prospektiv angelegte klinische Studien wünschenswert, um das klinische Langzeitverhalten dieser neuen Werkstoffe zu prüfen.

Allerdings kann erwartet werden, dass diese Herausforderungen in den kommenden Jahren mithilfe fortschreitender Forschungs- und Entwicklungsarbeit sowohl von überarbeiteten Drucktechnologien als auch verbesserten Materialien im Hinblick des digitalen Zeitalters effektiv bewerkstelligt werden.

6. Englische Zusammenfassung

On the basis of the investigations summarized here, it can be concluded that 3D printing using FLM technology of the high-performance polymer PEEK in dentistry has the potential to challenge traditional manufacturing processes. In particular, it will provide enormous competition to the already established subtractive manufacturing technology in the upcoming years.

Although printed standardized specimens showed worse Martens parameters than milled ones, there were no differences in the fracture load of printed and milled class I inlays, which were also above the occurring physiological and maximum masticatory forces. Furthermore, it can be observed that the printing direction and thus the orientation of the layers laid on top of each other has a relevant influence on the mechanical performance, in that positioning the printed layers perpendicular to the direction of loading provides the best mechanics.

While hydrothermal aging processes demonstrated a negative impact on the mechanics of the milled specimens in particular, chewing simulation showed no effect on the fracture load of restored teeth with indirect PEEK inlays, which may be encouraging for high clinical performance and long-term durability. A decisive disadvantage of the printed components is the required postprocessing and the still existing lack of knowledge about the exact composition and thermodynamic behavior of the PEEK filaments. Improvements in printing accuracy and aesthetics of the printed parts are also required to ensure that the high quality requirements in dentistry are achieved.

Although the investigations carried out have yielded promising results, the processing of PEEK using additive technology in dentistry is still a challenge due to the high demands on mechanics, precision and aesthetics in order to be able to be used successfully in vivo as an alternative biocompatible material using this production process. Beyond this background prospective long-term clinical studies are necessary to evaluate the clinical performance.

However, it can be expected that this challenge will be effectively managed in the coming years through ongoing research and development of revised printing technologies as well as improved materials with regard to the digital age.

7. Literaturverzeichnis

[1] Ngo TD, Kashani A, Imbalzano G, Nguyen KTQ, Hui D. Additive manufacturing (3D printing): a review of materials, methods, applications and challenges. Compos B Eng 2018;143:172-96.

[2] van Noort R. The future of dental devices is digital. Dent Mater 2012;28:3-12.

[3] Dimitrov D, Schreve K, de Beer N. Advances in three dimensional printing - state of the art and future perspectives. Rapid Prototyp J 2006;12:136-47.

[4] Barazanchi A, Li KC, Al-Amleh B, Lyons K, Waddell JN. Additive technology: update on current materials and applications in dentistry. J Prosthodont 2017;26:156-63.

[5] Galante R, Figueiredo-Pina CG, Serro AP. Additive manufacturing of ceramics for dental applications: A review. Dent Mater 2019;35:825-46.

[6] Revilla-León M, Özcan M. Additive manufacturing technologies used for processing polymers: current status and potential application in prosthetic dentistry. J Prosthodont 2019;28:146-58.

[7] Valentan B, Kadivnik Z, Brajlih T, Anderson A, Igor D. Processing poly(ether etherketone) on a 3d printer for thermoplastic modelling. Mater Technol 2013;47:715-21.

[8] Mishra S, Chowdhary R. PEEK materials as an alternative to titanium in dental implants: A systematic review. Clin Implant Dent Relat Res 2019;21:208-22.

[9] Maekawa M, Kanno Z, Wada T, Hongo T, Doi H, Hanawa T, et al. Mechanical properties of orthodontic wires made of super engineering plastic. Dent Mater J 2015;34:114-9.

[10] Kurtz SM, Devine JN. PEEK biomaterials in trauma, orthopedic, and spinal implants. Biomaterials 2007;28:4845-69.

[11] Shahdad SA, McCabe JF, Bull S, Rusby S, Wassell RW. Hardness measured with traditional Vickers and Martens hardness methods. Dent Mater 2007;23:1079-85.

[12] Quinn JB, Quinn GD. A practical and systematic review of Weibull statistics for reporting strengths of dental materials. Dent Mater 2010;26:135-47.

[13] Rosentritt M, Behr M, van der Zel JM, Feilzer AJ. Approach for valuating the influence of laboratory simulation. Dent Mater 2009;25:348-52.

[14] Oberoi G, Nitsch S, Edelmayer M, Janjić K, Müller AS, Agis H. 3D Printing - encompassing the facets of dentistry. Front Bioeng Biotechnol 2018;6:172.

[15] Liaw C-Y, Guvendiren M. Current and emerging applications of 3D printing in medicine. Biofabrication 2017;9:024102.

[16] Tack P, Victor J, Gemmel P, Annemans L. 3D-printing techniques in a medical setting: a systematic literature review. Biomed Eng Online 2016;15:115.

[17] Wang X, Jiang M, Zhou Z, Gou J, Hui D. 3D printing of polymer matrix composites: a review and prospective. Compos B Eng 2017;110:442-58.

[18] Katzer A, Marquardt H, Westendorf J, Wening JV, von Foerster G. Polyetheretherketone - cytotoxicity and mutagenicity in vitro. Biomaterials 2002;23:1749-59.

[19] Poulsson AH, Eglin D, Zeiter S, Camenisch K, Sprecher C, Agarwal Y, et al. Osseointegration of machined, injection moulded and oxygen plasma modified PEEK implants in a sheep model. Biomaterials 2014;35:3717-28.

[20] Toth JM, Wang M, Estes BT, Scifert JL, Seim HB, Turner AS. Polyetheretherketone as a biomaterial for spinal applications. Biomaterials 2006;27:324-34.

[21] Maldonado-Naranjo AL, Healy AT, Kalfas IH. Polyetheretherketone (PEEK) intervertebral cage as a cause of chronic systemic allergy: a case report. Spine J 2015;15:e1-3.

[22] Zoidis P, Bakiri E, Polyzois G. Using modified polyetheretherketone (PEEK) as an alternative material for endocrown restorations: a short-term clinical report. J Prosthet Dent 2017;117:335-9.

[23] Tekin S, Cangül S, Adıgüzel Ö, Değer Y. Areas for use of PEEK material in dentistry. Int Dent Res 2018;8:84-92.

[24] Park C, Jun DJ, Park SW, Lim HP. Use of polyaryletherketone (PAEK) based polymer for implant-supported telescopic overdenture: a case report. J Adv Prosthodont 2017;9:74-6.

[25] Ali MZ, Baker S, Martin N. Traditional CoCr versus milled PEEK framework removable partial dentures-pilot randomised crossover controlled trial; interim findings. ConsEuro 2015. BM09 London.

[26] Schwitalla A, Müller WD. PEEK dental implants: a review of the literature. J Oral Implantol 2013;39:743-9.

[27] Stawarczyk B, Eichberger M, Uhrenbacher J, Wimmer T, Edelhoff D, Schmidlin PR. Three-unit reinforced polyetheretherketone composite FDPs: influence of fabrication method on load-bearing capacity and failure types. Dent Mater J 2015;34:7-12.

[28] Zhao F, Li D, Jin Z. Preliminary Investigation of poly-ether-Ether-Ketone based on fused deposition modeling for medical applications. Materials 2018;11.

[29] Deng X, Zeng Z, Peng B, Yan S, Ke W. Mechanical properties optimization of poly-ether-Ether-Ketone via fused deposition modeling. Materials 2018;11.

[30] Yang C, Tian X, Li D, Cao Y, Zhao F, Shi C. Influence of thermal processing conditions in 3D printing on the crystallinity and mechanical properties of PEEK material. J Mater Process Technol 2017;248:1-7.

[31] Wu W, Geng P, Li G, Zhao D, Zhang H, Zhao J. Influence of layer thickness and raster angle on the mechanical properties of 3D-Printed PEEK and a comparative mechanical study between PEEK and ABS. Materials 2015;8:5834-46.

[32] Rinaldi M, Ghidini T, Cecchini F, Brandao A, Nanni F. Additive layer manufacturing of poly (ether ether ketone) via FDM. Compos B Eng 2018;145:162-72.

[33] BS EN ISO 14577-1:2002(E): Metallic materials - Instrumented indentation test for hardness and materials parameters - part 1: Test method.77.040.10.

[34] Greaves GN, Greer AL, Lakes RS, Rouxel T. Poisson's ratio and modern materials. Nat Mater 2011;10:823-37.

[35] Hampe R, Lümkemann N, Sener B, Stawarczyk B. The effect of artificial aging on Martens hardness and indentation modulus of different dental CAD/CAM restorative materials. J Mech Behav Biomed Mater 2018;86:191-8.

[36] Bürgin S, Rohr N, Fischer J. Assessing degradation of composite resin cements during artificial aging by Martens hardness. Head Face Medicine 2017;13:9.

[37] Ullner C. Die Reihe DIN EN ISO 14577 - Erste weltweit akzeptierte Normen für die instrumentierte Eindringprüfung. Bundesanstalt für Materialforschung.

[38] Yang X, Wu Y, Wei K, Fang W, Sun H. Non-isothermal crystallization kinetics of short glass Fiber reinforced poly (Ether ether ketone) composites. Materials 2018;11:2094.

[39] Seo Y, Kim S. Nonisothermal crystallization behavior of poly(aryl ether ether ketone). Polym Eng Sci 2001;41:940-5.

[40] Alharbi N, Osman R, Wismeijer D. Effects of build direction on the mechanical properties of 3D-printed complete coverage interim dental restorations. J Prosthet Dent 2016;115:760-7.

[41] Puebla K, Arcaute K, Quintana R, Wicker RB. Effects of environmental conditions, aging, and build orientations on the mechanical properties of ASTM type I specimens manufactured via stereolithography. Rapid Prototyp J 2012;18:374-88.

[42] Panayotov IV, Orti V, Cuisinier F, Yachouh J. Polyetheretherketone (PEEK) for medical applications. J Mater Sci Mater Med 2016;27:118.

[43] Han X, Yang D, Yang C, Spintzyk S, Scheideler L, Li P, et al. Carbon Fiber reinforced PEEK composites based on 3D-Printing technology for orthopedic and dental applications. J Clin Med 2019;8:240.

[44] Morresi AL, D'Amario M, Capogreco M, Gatto R, Marzo G, D'Arcangelo C, et al. Thermal cycling for restorative materials: does a standardized protocol exist in laboratory testing? A literature review. J Mech Behav Biomed Mater 2014;29:295-308.

[45] Chevalier J. What future for zirconia as a biomaterial? Biomaterials 2006;27:535-43.

[46] Kumar A, Yap WT, Foo SL, Lee TK. Effects of sterilization cycles on PEEK for medical device application. Bioengineering 2018;5:18.

[47] Liebermann A, Wimmer T, Schmidlin PR, Scherer H, Löffler P, Roos M, et al. Physicomechanical characterization of polyetheretherketone and current esthetic dental CAD/CAM polymers after aging in different storage media. J Prosthet Dent 2016;115: 321-8.e2.

[48] Dawood A, Marti Marti B, Sauret-Jackson V, Darwood A. 3D printing in dentistry. Br Dent J 2015;219:521-9.

[49] Reymus M, Fotiadou C, Kessler A, Heck K, Hickel R, Diegritz C. 3D printed replicas for endodontic education. Int Endod J 2019;52:123-30.

[50] Javaid M, Haleem A. Current status and applications of additive manufacturing in dentistry: a literature-based review. J Oral Biol Craniofac Res 2019;9:179-85.

[51] Haleem A, Javaid M. Polyether ether ketone (PEEK) and its manufacturing of customised 3D printed dentistry parts using additive manufacturing. Clin Epidemiol Glob Health 2019;7:654-60.

[52] Bathala L, Majeti V, Rachuri N, Singh N, Gedela S. The role of polyether ether ketone (Peek) in dentistry - a review. J Med Life 2019;12:5-9.

[53] Vaezi M, Yang S. Extrusion-based additive manufacturing of PEEK for biomedical applications. Virtual and Physical Prototyping 2015;10:123-35.

[54] Mondelli J, Sene F, Ramos RP, Benetti AR. Tooth structure and fracture strength of cavities. Braz Dent J 2007;18:134-8.

[55] Larson TD, Douglas WH, Geistfeld RE. Effect of prepared cavities on the strength of teeth. Oper Dent 1981;6:2-5.

[56] Coelho-de-Souza FH, Camacho GB, Demarco FF, Powers JM. Fracture resistance and gap formation of MOD restorations: influence of restorative technique, bevel preparation and water storage. Oper Dent 2008;33:37-43.

[57] Bütikofer L, Stawarczyk B, Roos M. Two regression methods for estimation of a two-parameter Weibull distribution for reliability of dental materials. Dent Mater 2015;31:e33-e50.

[58] Geigy WT. Statistik T vol. 8. 1980. CIBA-GEIGY Limited, Basel.

[59] Fontijn-Tekamp FA, Slagter AP, Van Der Bilt A, Van THMA, Witter DJ, Kalk W, et al. Biting and chewing in overdentures, full dentures, and natural dentitions. J Dent Res 2000;79:1519-24.

[60] Helkimo E, Carlsson G, Helkimo M. Bite force and state dentition. Acta Odontol Scand 1977;35:297-303.

[61] Waltimo A, Könönen M. Maximal bite force and its association with signs and symptoms of craniomandibular disorders in young Finnish non-patients. Acta Odontol Scand 1995;53:254-8.

[62] Ahlberg JP, Kovero OA, Hurmerinta KA, Zepa I, Nissinen MJ, Könönen MH. Maximal bite force and its association with signs and symptoms of TMD, occlusion, and body mass index in a cohort of young adults. Cranio 2003;21:248-52.

[63] Aggarwal V, Logani A, Jain V, Shah N. Effect of cyclic loading on marginal adaptation and bond strength in direct vs. indirect class II MO composite restorations. Oper Dent 2008;33:587-92.

[64] Mondelli J, Steagall L, Ishikiriama A, de Lima Navarro MF, Soares FB. Fracture strength of human teeth with cavity preparations. J Prosthet Dent 1980;43:419-22.

[65] Reeh ES, Messer HH, Douglas WH. Reduction in tooth stiffness as a result of endodontic and restorative procedures. J Endod 1989;15:512-6.

[66] Lubisich EB, Hilton TJ, Ferracane J. Cracked Teeth: a review of the literature. J Esthet Restor Dent 2010;22:158-67.

[67] Watts DC. Elastic moduli and visco-elastic relaxation. J Dent 1994;22:154-8.

[68] Habelitz S, Marshall SJ, Marshall GW, Balooch M. Mechanical properties of human dental enamel on the nanometre scale. Arch Oral Biol 2001;46:173-83.

[69] Costa AKF, Xavier TA, Noritomi PY, Saavedra G, Borges ALS. The influence of elastic modulus of inlay materials on stress distribution and fracture of premolars. Oper Dent 2014;39:E160-70.

[70] Melo RA, Bispo AdSL, Barbosa GAS, Galvão MR, de Assunção IV, Souza ROdA, et al. Morphochemical characterization, microhardness, water sorption, and solubility of regular viscosity bulk fill and traditional composite resins. Microsc Res Tech 2019;82:1500-6.

[71] Sheen C-Y, Dong J-K, Brantley WA, Han DS. A study of fracture loads and fracture characteristics of teeth. J Adv Prosthodont 2019;11:187-92.

[72] Shetty M, Rajalakshmi S, Krishna Prasad D. Comparison of marginal gap and microleakage in copy-milled and cad-milled zirconia copings bonded using light cure and chemical cure resin bonding systems. J Indian Prosthodont Soc 2014;14:37-45.

[73] Okutan M, Heydecke G, Butz F, Strub JR. Fracture load and marginal fit of shrinkage-free ZrSiO4 all-ceramic crowns after chewing simulation. J Oral Rehabil 2006;33:827-32.

[74] Taufall S, Eichberger M, Schmidlin PR, Stawarczyk B. Fracture load and failure types of different veneered polyetheretherketone fixed dental prostheses. Clin Oral Investig 2016;20:2493-2500.

[75] Uhrenbacher J, Schmidlin PR, Keul C, Eichberger M, Roos M, Gernet W, et al. The effect of surface modification on the retention strength of polyetheretherketone crowns adhesively bonded to dentin abutments. J Prosthet Dent 2014;112:1489-97.

[76] Stawarczyk B, Taufall S, Roos M, Schmidlin PR, Lümkemann N. Bonding of composite resins to PEEK: the influence of adhesive systems and air-abrasion parameters. Clin Oral Investig 2018;22:763-71.

[77] Frankenberger R, Krämer N, Appelt A, Lohbauer U, Naumann M, Roggendorf MJ. Chairside vs. labside ceramic inlays: effect of temporary restoration and adhesive luting on enamel cracks and marginal integrity. Dent Mater 2011;27:892-8.

[78] Liebermann A, Ilie N, Roos M, Stawarczyk B. Effect of storage medium and aging duration on mechanical properties of self-adhesive resin-based cements. J Appl Biomater Funct Mater 2017;15:e206-14.

[79] Wafaie RA, Ibrahim Ali A, Mahmoud SH. Fracture resistance of prepared premolars restored with bonded new lab composite and all-ceramic inlay/onlay restorations: laboratory study. J Esthet Restor Dent 2018;30:229-39.

8. Danksagung

Ich bedanke mich bei all denjenigen, die mich tatkräftig bei meiner Dissertation unterstützt und motiviert haben. Ein besonderes Dankeschön haben sich folgende Personen verdient:

- Prof. Dr. Dipl.-Ing. (FH) Bogna Stawarczyk, M.Sc. als Mitglied der Betreuungskommission für die Überlassung des Themas und ihre ausgezeichnete fachkundliche und liebevolle Unterstützung.
- Dr. med. dent. Marcel Reymus für seine immer hilfsbereite freundschaftliche Betreuung.
- Dr.-Ing. Miriam Haerst, Stefan Leonhardt, Sebastian Pammer und Stefan Fischer von dem Unternehmen KUMOVIS für die Bereitstellung des 3D-Druckers, der PEEK-Filamente sowie die hervorragende technische Unterstützung.
- Prof. Dr. med. dent. Daniel Edelhoff als Mitglied der Betreuungskommission für die Möglichkeit der Durchführung der Studien und das Korrekturlesen der Manuskripte.
- Prof. Dr. med. dent. Reinhard Hickel als Mitglied der Betreuungskommission für die Möglichkeit der Durchführung der Studien und das Korrekturlesen der Manuskripte.
- ZT Marlis Eichberger für ihre zahntechnische Hilfestellung bei der Durchführung der Versuche im Labor.
- Alle Mitarbeiter und Doktoranden der Werkstoffkundeforschung der Poliklinik für Zahnärztliche Prothetik der LMU für die tolle kollegiale Zusammenarbeit.
- Besonderer Dank gebührt meinen Eltern, die mir während meiner gesamten Ausbildungszeit immer mit Rat und Tat zur Seite standen.